Inorg. Chem. **2009**, *48*, 2793−2807

Engineering New Metal-Organic Frameworks Built from Flexible Tetrapyridines Coordinated to Cu(II) and Cu(I)

Patrick E. Ryan, Christophe Lescop, Dominic Laliberté, Tamara Hamilton, Thierry Maris, and James D. Wuest*

Département de Chimie, Université de Montréal, Montréal, Québec H3C 3J7, Canada

Received October 16, 2008

A series of new metal-organic frameworks have been constructed by the coordination of Cu(II) and Cu(I) with pentaerythrityl tetrakis(4-pyridyl) ether (**1** = PETPE), a flexible tetradentate ligand. Networks derived from $Cu(OOCCH_3)_2$, $Cu(NO_3)_2$, and $CuBF_4$ proved to have different topologies (diamondoid, PtS, and $SrAl_2$, respectively). This reflects (1) the ability of PETPE (**1**) to adopt diverse conformations and (2) the varied geometries of complexes of Cu(II) and Cu(I). Extended PETPE (**2**), a tetrapyridine with phenyl spacers inserted into the pentaerythrityl core of PETPE (**1**), yielded an expanded version of the PtS network derived from simple PETPE (**1**) and $Cu(NO_3)_2$. However, increases in the ability of the network to accommodate guests were largely offset by interpenetration of independent networks. Attempts to thwart interpenetration by converting ligand **2** into methyl-substituted derivative **3** led to the construction of networks with alternative topologies. In particular, the reactions of ligand **3** with both Cu(II) and Cu(I) yielded isostructural Pt_3O_4 networks, despite the preference of the two oxidation states for coordination spheres with different geometries. Together, these observations demonstrate that PETPE (**1**) and related compounds are useful ligands for constructing metal-organic frameworks, with a distinctive ability to accommodate a single metal in different oxidation states, as well as to adapt to a metal in a single oxidation state but with different counterions or secondary ligands.

Introduction

A major challenge in science today is to learn how to prepare new molecular materials with predetermined structures and properties. Reaching this objective will require advances in basic science, and it will create opportunities for breakthroughs in many areas of technology. Unfortunately, developing the necessary understanding remains an elusive goal, in part because the forces that position molecules and help determine their collective properties are complex and hard to control. In general, the structures and properties of materials are impossible to predict reliably, even when the most powerful current computational techniques are used.[1]

Nevertheless, important progress is being made in the effort to create new molecular materials by design. In particular, noteworthy advances have occurred in the field of engineering crystalline materials built from carefully selected molecular components. This work has demonstrated that molecular subunits for the purposeful construction of crystalline materials are particularly effective when they have the following features: (1) They incorporate multiple sites of strong directional intermolecular interactions; and (2) they hold these sites in particular orientations that favor the assembly of networks in which each molecule is positioned predictably with respect to its neighbors.[2−4] Interactions that have proven to be especially suitable for engineering crystalline materials of this type include hydrogen bonds and coordinative bonds to metals. Many simple functional groups that engage in reliable motifs of hydrogen bonding or coordination to metals can be incorporated in molecules with

* To whom correspondence should be addressed. E-mail: james.d.wuest@umontreal.ca.

(1) For examples of recent efforts to use ab initio methods to predict the structures and properties of molecular crystals, see: Neumann, M. A.; Leusen, F. J. J.; Kendrick, J. *Angew. Chem., Int. Ed.* **2008**, *47*, 2427–2430. Misquitta, A. J.; Welch, G. W. A.; Stone, A. J.; Price, S. L. *Chem. Phys. Lett.* **2008**, *456*, 105–109. Trolliet, C.; Poulet, G.; Tuel, A.; Wuest, J. D.; Sautet, P. *J. Am. Chem. Soc.* **2007**, *129*, 3621–3626.

(2) For recent references to studies of molecular networks held together by hydrogen bonds, see: Wuest, J. D. *Chem. Commun.* **2005**, 5830–5837. Hosseini, M. W. *Acc. Chem. Res.* **2005**, *38*, 313–323.

10.1021/ic8019809 CCC: $40.75
Published on Web 03/09/2009

diverse geometries, thereby creating countless opportunities to make new crystalline materials with different compositions, architectures, and properties.

Close conceptual analogies exist between molecular networks held together by coordinative interactions with metals, which can have a significant degree of covalent character, and networks maintained by non-covalent interactions such as hydrogen bonds. Despite underlying similarities, however, development of the two classes of materials has tended to occur within the separate confines of inorganic chemistry and organic chemistry. This approach has emphasized how the materials are different, rather than how they are alike. These circumstances create an attractive opportunity to engineer new crystalline materials using an integrated approach in which understanding of inorganic chemistry and organic chemistry plays equally important roles.

To test the ability of this hybrid approach to yield new insights, we have begun to explore the coordination chemistry of pentaerythrityl tetrakis(4-pyridyl) ether (**1**),[5] which will be referred to as PETPE. PETPE is a flexible tetradentate

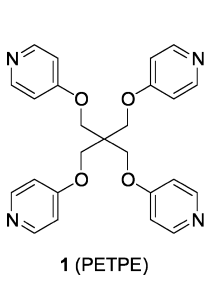

1 (PETPE)

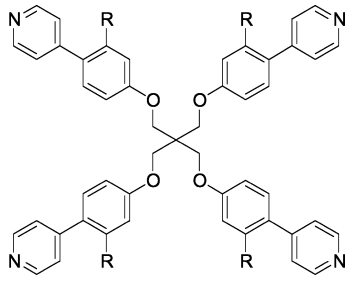

2 (R = H)
3 (R = CH_3)

ligand that has not previously been used to bind metals. In addition, we have subjected its structure to rational modifications designed to produce metal-organic frameworks with new features. In particular, phenyl spacers were inserted into the pentaerythrityl core of PETPE (**1**) to create analogue **2**, a precursor of expanded frameworks, and substituted extended derivative **3** was prepared to thwart intermolecular aromatic interactions and thereby alter molecular packing. In this paper, we report the structures and properties of a series of nine complexes produced when ligands **1**−**3** bind Cu(II) and Cu(I),[6] and we will describe the coordination of

Scheme 1

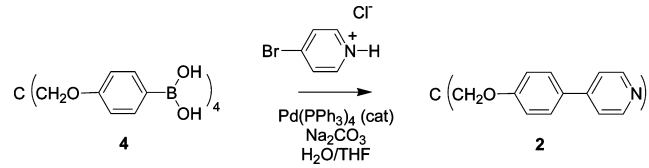

Scheme 2

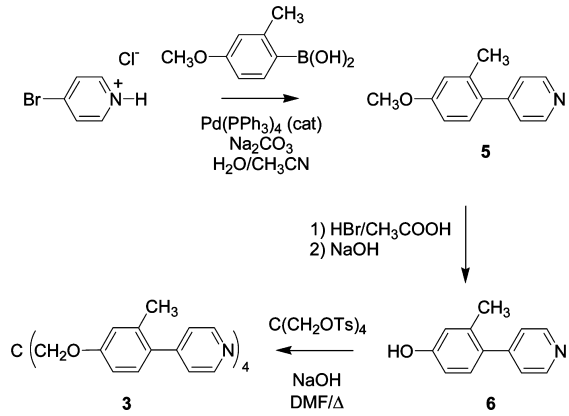

other metals in the future. Our work blends inorganic chemistry and organic chemistry in equal measure, and the results illustrate how studies in which coordination chemistry is combined with sophisticated molecular design and synthesis can be productive sources of new insights and hybrid materials with unusual properties.

Results and Discussion

Synthesis of Tetrapyridines 1−3. PETPE (**1**) was previously prepared by converting pentaerythritol into the corresponding tetratosylate,[7] which was then heated with 4-hydroxypyridine in the presence of base.[5] We prepared tetrapyridine **1** in 86% yield in a single step by treating 4-chloropyridinium chloride with pentaerythritol in the presence of excess KOH. Extended PETPE (**2**) was synthesized in 73% yield by Suzuki coupling of the previously reported tetraboronic acid **4**[8] with 4-bromopyridine (Scheme 1). By the route summarized in Scheme 2, substituted extended analogue **3** was synthesized in three steps in an overall yield of 54%. Suzuki coupling of 4-bromopyridine with (4-methoxy-2-methylphenyl)boronic acid provided 4-(4-methoxy-2-methylphenyl)pyridine (**5**) in 85% yield. Demethylation of intermediate **5** under standard conditions (HBr/CH_3COOH) occurred in 70% yield to give the corresponding phenol **6**,[9] which was converted into target compound **3** in 90% yield by treatment with pentaerythrityl tetratosylate[7] in the presence of NaOH.

Structures of Networks Produced by Treating PETPE (1) with $Cu(OOCCH_3)_2$, $Cu(NO_3)_2$, and $CuBF_4$. Slow mixing of an ethanolic solution of tetrapyridine **1** with a methanolic solution of $Cu(OOCCH_3)_2$ produced deep blue

(3) For recent references to studies of networks linked by coordination to metals, see: Shimizu, G. K. H. *J. Solid State Chem.* **2005**, *178*, 2519–2526. Hill, R. J.; Long, D.-L.; Champness, N. R.; Hubberstey, P.; Schröder, M. *Acc. Chem. Res.* **2005**, *38*, 337–350. Férey, G.; Mellot-Draznieks, C.; Serre, C.; Millange, F. *Acc. Chem. Res.* **2005**, *38*, 217–225. Ockwig, N. W.; Delgado-Friedrichs, O.; O'Keeffe, M.; Yaghi, O. M. *Acc. Chem. Res.* **2005**, *38*, 176–182. Kitigawa, S.; Uemura, K. *Chem. Soc. Rev.* **2005**, *34*, 109–119. Rosseinsky, M. J. *Microporous Mesoporous Mater.* **2004**, *73*, 15–30. Janiak, C. *Dalton Trans* **2003**, 2781–2804. James, S. L. *Chem. Soc. Rev.* **2003**, *32*, 276–288. Robson, R. *J. Chem. Soc., Dalton Trans.* **2000**, 3735–3744.

(4) Brammer, L. *Chem. Soc. Rev.* **2004**, *33*, 476–489. Moulton, B.; Zaworotko, M. J. *Chem. Rev.* **2001**, *101*, 1629–1658.

(5) St. Pourcain, C. B.; Griffin, A. C. *Macromolecules* **1995**, *28*, 4116–4121.

(6) For a review of the coordination chemistry of Cu, see: Hathaway, B. J. In *Comprehensive Coordination Chemistry*; Wilkinson, G., Gillard, R. D., McCleverty, J. A., Eds.; Pergamon: Oxford, 1987; Vol. *5*, pp 533−594.

(7) Shostakovskii, M. F.; Atavin, A. S.; Mirskova, A. N. *Zh. Obshch. Khim.* **1965**, *35*, 804–807.

(8) Laliberté, D.; Maris, T.; Wuest, J. D. *J. Org. Chem.* **2004**, *69*, 1776–1787.

(9) Diemer, V.; Chaumeil, H.; Defoin, A.; Fort, A.; Boeglin, A.; Carré, C. *Eur. J. Org. Chem.* **2006**, 2727–2738.

Table 1. Crystallographic Data for Complexes of PETPE (**1**) with Salts of Cu(II) and Cu(I)

complex with	$Cu(OOCCH_3)_2$	$Cu(NO_3)_2$	$CuBF_4$
solvent of crystallization	$CH_3CH_2OH/CH_3OH/H_2O$	CH_3CH_2OH/H_2O	CH_2Cl_2/CH_3CN
crystal system	tetragonal	orthorhombic	monoclinic
space group	$I4_1/a$	*Cccm*	*C*2/*c*
a (Å)	22.782(3)	9.0229(3)	14.272(2)
b (Å)	22.782(3)	21.6107(8)	24.516(4)
c (Å)	9.804(12)	24.0491(9)	21.640(3)
β (deg)	90	90	97.075(4)
V (Å^3)	5089(2)	4689.4(3)	7514.0(19)
D_{calc} (g cm^{-3})	1.431	1.406	1.292
Z	4	4	4
temperature (K)	290(2)	223(2)	223(2)
unique	2409	2404	7145
observed ($I > 2\sigma(I)$)	2396	2061	7085
parameters	154	149	458
restraints	2	7	19
$R_1{}^a(I > 2\sigma(I))$	0.0792	0.0940	0.0781
$wR_2{}^b(I > 2\sigma(I))$	0.1819	0.2219	0.1828
$R_1{}^a$(all data)	0.0932	0.0945	0.0849
$wR_2{}^b$(all data)	0.2115	0.2226	0.2321
GoF^c	0.947	1.138	1.106

^{a} $R_1 = \sum||F_o| - |F_c||/\sum|F_o|$. ^{b} $wR_2 = \{\sum[w(F_o^2 - F_c^2)^2]/\sum w(F_o^2)^2\}^{1/2}$. ^{c} GoF $= \{\sum[w(F_o^2 - F_c^2)^2]/(n - p)\}^{1/2}$, where *n* is the number of reflections and *p* is the total number of parameters refined.

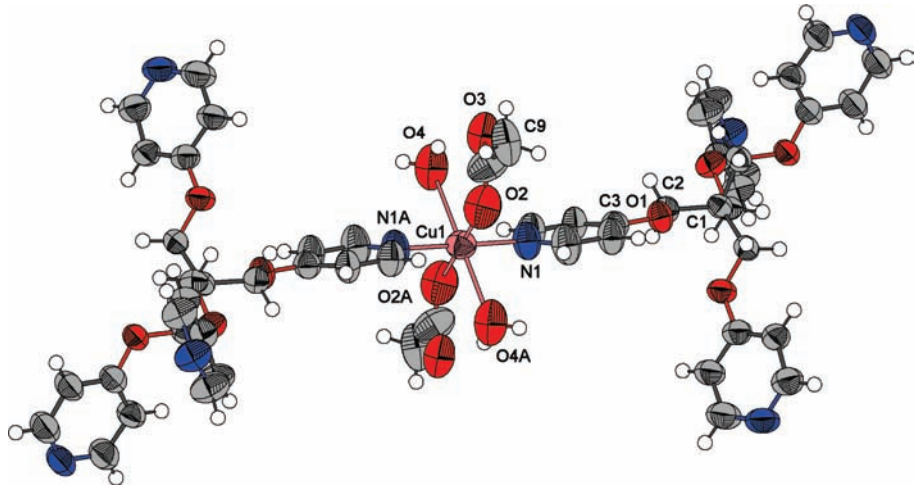

Figure 1. Partial view of the structure of crystals of the complex of $Cu(OOCCH_3)_2$ and PETPE (**1**) grown from $CH_3CH_2OH/CH_3OH/H_2O$. Thermal displacement ellipsoids are drawn at the 50% probability level, and hydrogen atoms are represented by a sphere of arbitrary size. Atoms of hydrogen appear in white, carbon in gray, nitrogen in blue, oxygen in red, and Cu(II) in bronze. Molecules of guests not bonded to Cu(II) are omitted. Key bond lengths include Cu1−N1 = 2.0168(9) Å, Cu1−O2 = 1.9732(13) Å, and Cu1−O4 = 2.589(1) Å.

crystals suitable for analysis by X-ray diffraction. The crystals proved to have the approximate composition $[Cu_2(\mathbf{1})(OOCCH_3)_4(H_2O)_4]\cdot 20H_2O$.[10] Crystallographic data appear in Table 1, and views of the structure are shown in Figures 1−3. Figure 1 reveals that the coordination sphere of Cu(II) is approximately octahedral, with bond angles in the range 86.67(5)−93.33(5)° and *trans*-oriented pairs of bound pyridyl groups, water, and monodentate acetate. Observed lengths for the Cu−N and Cu−O bonds are similar to those found in related complexes of Cu(II).[11] Pronounced lengthening of the diaxial C−OH_2 bonds is a manifestation of Jahn−Teller distortion, a characteristic structural feature resulting from the d^9 electronic configuration of Cu(II).[12]

In its complex with $Cu(OOCCH_3)_2$, inherently flexible ligand **1** adopts a conformation that holds four pyridyl groups in a highly distorted tetrahedral orientation. The distortion can be assessed by comparing the N···C_{core}···N angles defined by the central carbon atom of the pentaerythrityl core (C_{core}) and the nitrogen atoms of the pyridyl groups. These angles are 4 × 124.58(6)° and 2 × 82.23(6)°, showing that ligand **1** deviates significantly from tetrahedral geometry. Similar distortions have been observed in other pentaerythrityl tetraaryl ethers.[8,13] The −CH_2O− spacers that connect each pyridyl group to the core adopt conformations that are nearly fully extended, with C_{core}−CH_2−O−C dihedral angles

(10) The indicated composition shows only those components of the crystal that were at least partially ordered and were identified unambiguously by X-ray diffraction. The crystal also includes an undetermined amount of disordered guests.

(11) Marin, G.; Andruh, M.; Madalan, A. M.; Blake, A. J.; Wilson, C.; Champness, N. R.; Schröder, M. *Cryst. Growth Des.* **2008**, *8*, 964–975. Du, M.; Jiang, X.-J.; Zhao, X.-J.; Cai, H.; Ribas, J. *Eur. J. Inorg. Chem.* **2006**, 1245–1254. Chan, C.-W.; Mingos, D. M. P.; White, A. J. P.; Williams, D. J. *Polyhedron* **1996**, *15*, 1753–1767. Cameron, A. F.; Taylor, D. W.; Nuttal, R. H. *J. Chem. Soc., Dalton Trans.* **1972**, 1603–1608.

(12) Cotton, F. A.; Wilkinson, G.; Murillo, C. A.; Bochmann, M. *Advanced Inorganic Chemistry*; Wiley-Interscience: New York, 1999, pp. 854−876.

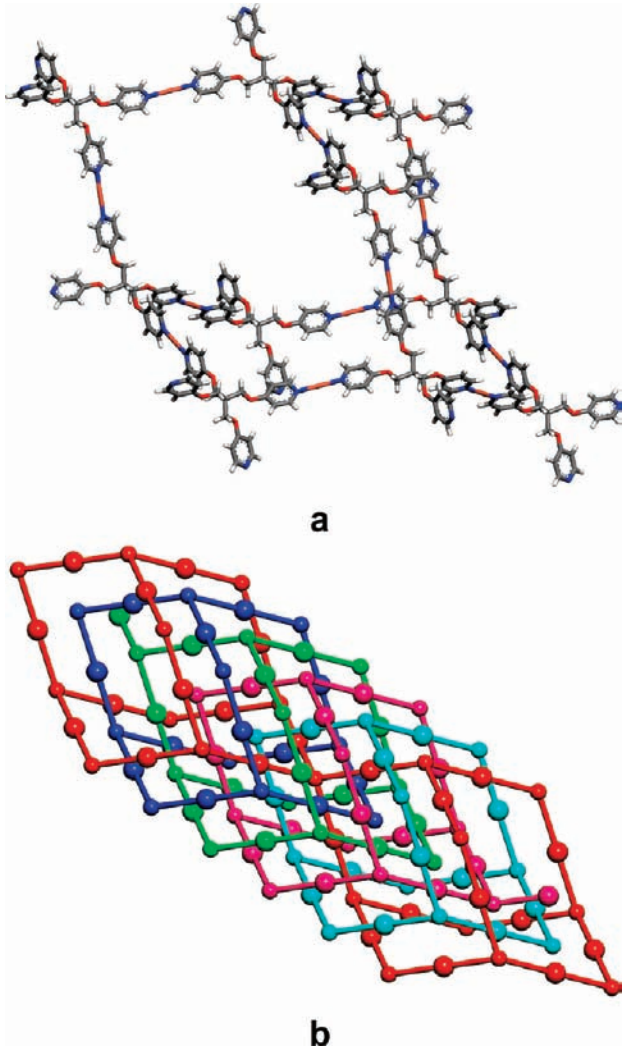

Figure 2. (a) Partial view of the distorted diamondoid network found in crystals of the complex of $Cu(OOCCH_3)_2$ and PETPE (**1**) grown from $CH_3CH_2OH/CH_3OH/H_2O$. Atoms of hydrogen appear in white, carbon in gray, nitrogen in blue, oxygen in red, and Cu(II) in bronze. Acetate and H_2O bound to Cu(II) are omitted for clarity, as are uncoordinated guests. (b) Representation of the 5-fold interpenetration of networks, with nodes (small spheres) and linkers (large spheres) corresponding to the central carbon atom of the pentaerythrityl core of ligand **1** and to Cu(II), respectively.

of 174.65(6)°. However, this extension does not continue across the central carbon atom (C_{core}), and the key $CH_2-C_{core}-CH_2-O$ dihedral angles are 70.16(4)°.

Binding of PETPE (**1**) to Cu(II) thereby defines a three-dimensional network that has a distorted diamondoid architecture, as shown in Figure 2a. Within this network, the central carbon atoms of ligands that share a common atom of Cu are separated by an intertectonic $C_{core}\cdots C_{core}$ distance of 16.731(4) Å. As a result, the network is open enough to accommodate 5-fold interpenetration (Figure 2b).[14] Despite this interpenetration, approximately 62% of the volume of the crystals remains accessible to guests, as measured by

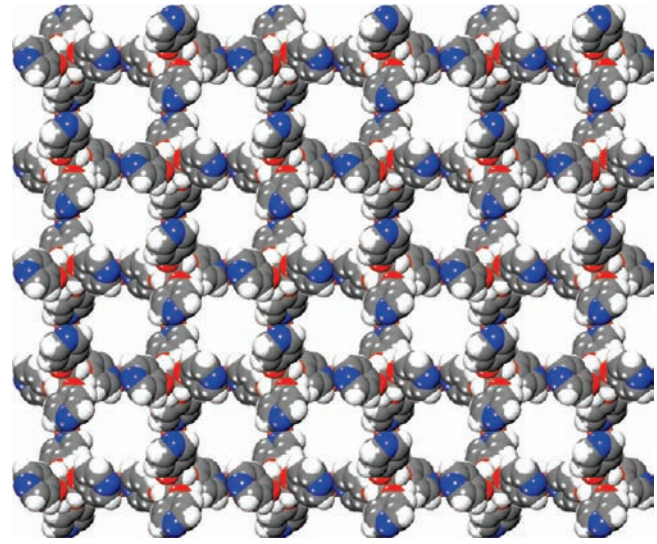

Figure 3. Representation of the structure of crystals of the complex of $Cu(OOCCH_3)_2$ and PETPE (**1**) grown from $CH_3CH_2OH/CH_3OH/H_2O$. The structure is viewed along the *c* axis and shows a $3 \times 3 \times 3$ array of unit cells. Acetate and H_2O bound to Cu(II) are omitted for clarity, as are uncoordinated guests. Atoms are represented by spheres of van der Waals radii to show the cross sections of the channels. Atoms of hydrogen appear in white, carbon in gray, nitrogen in blue, oxygen in red, and Cu(II) in bronze.

standard methods.[15−17] The guests occupy parallel channels that run along the *c* axis and have cross sections that are approximately 8.5×8.5 Å^2 (Figure 3).[18]

To assess the effect of replacing acetate by another anion, we allowed an ethanolic solution of PETPE (**1**) to mix slowly with an aqueous solution of $Cu(NO_3)_2$. This yielded violet crystals suitable for analysis by X-ray diffraction. The crystals were found to have the approximate composition $[Cu(\mathbf{1})(NO_3)_2]\cdot 20H_2O$.[10] Crystallographic data are provided in Table 1, and views of the structure appear in Figures 4−6. Figure 4 reveals that Cu(II) binds four pyridyl groups contributed by different molecules of ligand **1**, yielding a distorted octahedral metal center with N−Cu−N angles of $2 \times 88.73(15)°$ and $2 \times 90.42(15)°$ and Cu−N bonds of normal length.[11] Two nitrate ions that are 2-fold disordered

(13) Laliberté, D.; Maris, T.; Ryan, P. E.; Wuest, J. D. *Cryst. Growth Des.* **2006**, *6*, 1335–1340. Laliberté, D.; Maris, T.; Demers, E.; Helzy, F.; Arseneault, M.; Wuest, J. D. *Cryst Growth Des.* **2005**, *5*, 1451–1456. Laliberté, D.; Maris, T.; Wuest, J. D. *CrystEngComm* **2005**, *7*, 158–160. Laliberté, D.; Raymond, N.; Maris, T.; Wuest, J. D. *Acta Crystallogr.* **2005**, *E61*, o601−o603.

(14) For discussions of interpenetration in networks, see: Batten, S. R. *CrystEngComm* **2001**, *3*, 76–82. Batten, S. R.; Robson, R. *Angew. Chem., Int. Ed.* **1998**, *37*, 1460–1494.

(15) We estimate the percentage of volume accessible to guests by using the PLATON program.[16] PLATON calculates the accessible volume by allowing a spherical probe of variable radius to roll over the van der Waals surface of the network. PLATON uses a default value of 1.20 Å for the radius of the probe, which is an appropriate model for small guests such as water. The van der Waals radii used to define surfaces for these calculations are as follows: C, 1.70 Å; H, 1.20 Å; N, 1.55 Å; O, 1.52 Å; and Cu, 2.32 Å. If *V* is the volume of the unit cell and V_g is the guest-accessible volume as calculated by PLATON, then the porosity *P* in % is given by $100V_g/V$.

(16) Spek, A. L. *PLATON, A Multipurpose Crystallographic Tool*; Utrecht University: Utrecht, The Netherlands, 2001. van der Sluis, P.; Spek, A. L. *Acta Crystallogr.* **1990**, *A46*, 194–201.

(17) To allow related structures to be compared, the excluded volume was considered to be that occupied only by Cu and the bound tetrapyridines **1**−**3**. Other ligands, uncoordinated anions, and unbound neutral guests were all considered to occupy potentially accessible volume.

(18) The dimensions of a channel in a particular direction correspond to those of an imaginary cylinder that could be passed through the hypothetical open network in the given direction in contact with the van der Waals surface. These dimensions give the cross section at the most narrow constriction, and they no not fully reflect the porosity of networks with channels that are not uniform and linear.

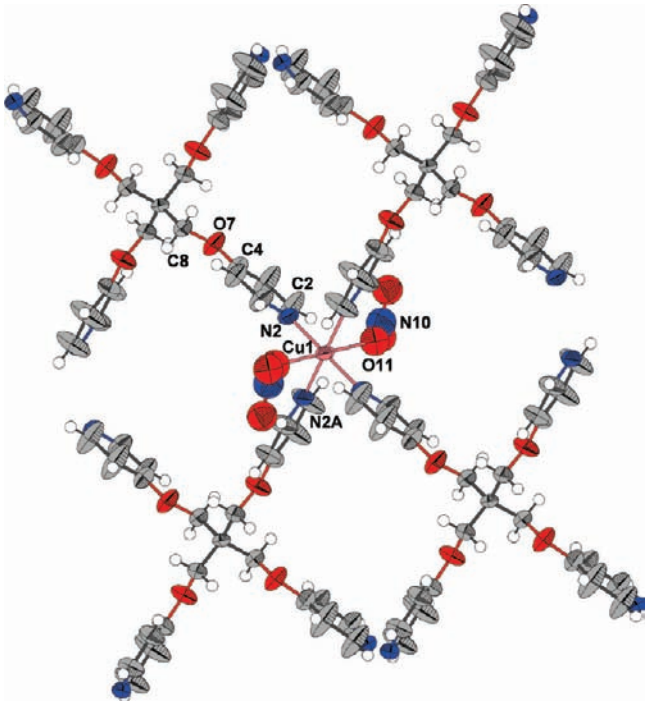

Figure 4. Partial view of the structure of crystals of the complex of $Cu(NO_3)_2$ and PETPE (**1**) grown from CH_3CH_2OH/H_2O. Thermal displacement ellipsoids are drawn at the 50% probability level, and hydrogen atoms are represented by a sphere of arbitrary size. Only two orientations of the disordered nitrates are displayed, and molecules of guests are omitted. Atoms of hydrogen appear in white, carbon in gray, nitrogen in blue, oxygen in red, and Cu(II) in bronze. Key bond lengths include Cu1−N2 = 2.036(3) Å and Cu1−O11 = 2.628(6) Å.

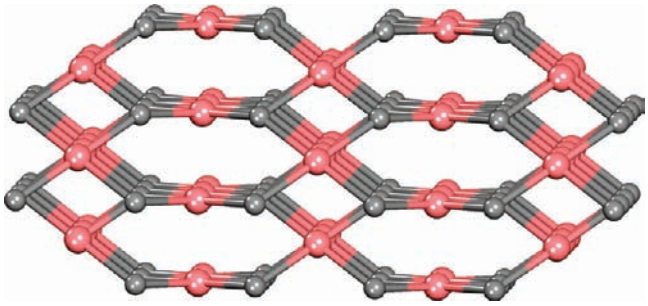

Figure 5. Representation of the PtS network found in crystals of the complex of $Cu(NO_3)_2$ and PETPE (**1**) grown from CH_3CH_2OH/H_2O. Nodes in the network correspond to the central carbon atom of ligand **1** (gray spheres) and to Cu(II) (bronze spheres).

complete the sphere of coordination of Cu(II), with C−O bonds elongated by Jahn−Teller distortion.[12]

The conformation adopted by PETPE (**1**) is substantially different from the one observed in its complex with $Cu(OOCCH_3)_2$. Again, the $-CH_2O-$ spacers that connect each pyridyl group to the core adopt conformations that are nearly fully extended, with $C_{core}-CH_2-O-C$ dihedral angles of −176.6(3)°. In the complex with $Cu(NO_3)_2$, however, this extension continues across the central carbon atom (C_{core}), giving two almost fully extended $C-O-CH_2-C_{core}-CH_2-O-C$ chains that lie in orthogonal planes. As a result, ligand **1** adopts a flattened conformation in which the $N\cdots C_{core}\cdots N$ angles are 2 × 88.68(4)°, 2 × 97.85(4)°, and 2 × 152.48(4)°.

In combination, the characteristic flattened geometry of PETPE (**1**) and the square-planar arrangement of pyridyl groups in the coordination sphere of Cu(II) give rise to an

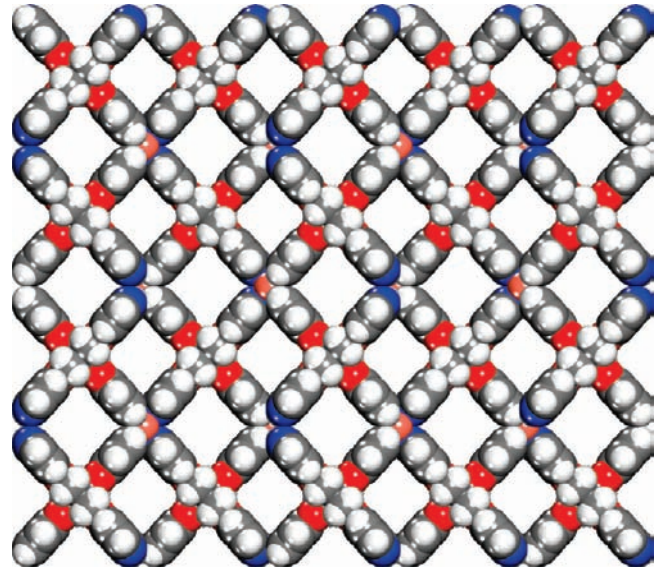

Figure 6. Representation of the structure of crystals of the complex of $Cu(NO_3)_2$ and PETPE (**1**) grown from CH_3CH_2OH/H_2O. The structure is viewed along the *a* axis and shows a 2 × 2 × 3 array of unit cells. Nitrate and neutral guests are omitted for clarity, and atoms are represented by spheres of van der Waals radii to show the cross sections of the channels. Atoms of hydrogen appear in white, carbon in gray, nitrogen in blue, oxygen in red, and Cu(II) in bronze.

open PtS network (Figure 5).[19,20] In this network, the central carbon atoms of adjacent ligands bonded to a common atom of Cu are separated by an intertectonic $C_{core}\cdots C_{core}$ distance of 16.784(9) Å, and the Cu···Cu distance spanned by a single ligand is 16.166(9) Å. No interpenetration is observed. The resulting network defines parallel channels that run along the *a* axis and have cross sections of approximate dimensions 6.4 × 7.3 $Å^2$ (Figure 6).[18] Approximately 63% of the volume of the crystals is accessible to disordered nitrate and neutral guests.[15−17]

Together, these results show how alterations of the coordination sphere of Cu(II) can be accommodated by the intrinsic flexibility of tetrapyridine **1**, which is able to produce highly open networks with distinctly different architectures. To induce further alterations, we replaced Cu(II) by Cu(I), which often displays a tetrahedral arrangement of ligands.[6] Slow mixing of a solution of PETPE (**1**) in CH_2Cl_2 with a solution of $Cu(CH_3CN)_4BF_4$ in CH_3CN provided yellow crystals suitable for analysis by X-ray diffraction (Table 1, Figures 7−9). The crystals proved to have the approximate composition $[Cu(\mathbf{1})(BF_4)]\cdot 2CH_3CN\cdot 3H_2O$.[10] Figure 7 shows that Cu(I) binds four pyridyl groups provided by different molecules of ligand **1**, yielding a complex with a distorted tetrahedral geometry. The N−Cu−N angles range from 101.82(3)° to 122.78(2)°, and the average length of the

(19) For a description of a network of PtS topology prepared by the reaction of $Cu(NO_3)_2$ with a tetrapyridine related to ligand **1**, see: Nättinen, K. I.; Rissanen, K. *Inorg. Chem.* **2003**, *42*, 5126–5134.

(20) For references to other metal-organic frameworks that adopt the PtS topology, see: Zhao, H.; Qu, Z.-R.; Ye, Q.; Wang, X.-S.; Zhang, J.; Xiong, R.-G.; You, X.-Z. *Inorg. Chem.* **2004**, *43*, 1813–1815.

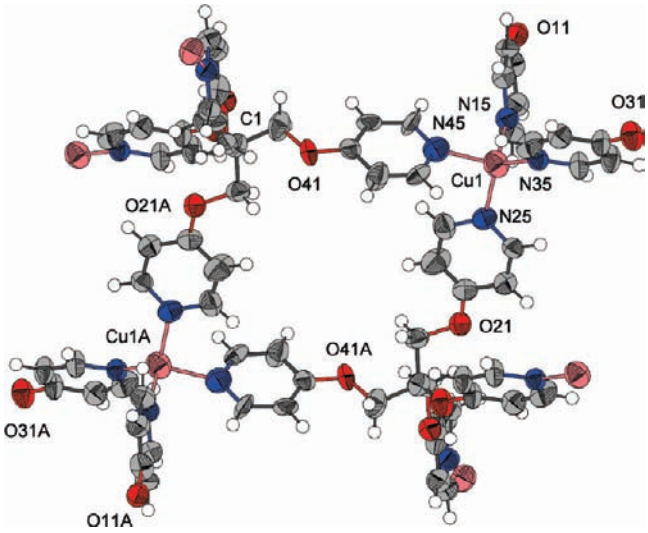

Figure 7. Partial view of the structure of crystals of the complex of $CuBF_4$ and PEPTE (**1**) grown from CH_2Cl_2/CH_3CN. Thermal displacement ellipsoids are drawn at the 50% probability level, and hydrogen atoms are represented by a sphere of arbitrary size. Atoms of hydrogen appear in white, carbon in gray, nitrogen in blue, oxygen in red, and Cu(I) in bronze. Anions and neutral guests are omitted. Key bond lengths include Cu1−N15 = 2.0833(7) Å, Cu1−N25 = 2.0091(6) Å, Cu1−N35 = 2.0095(6) Å, and Cu1−N45 = 2.1090(8) Å.

Cu−N bonds has a normal value (2.052(7) Å).[21] In its Cu(I) complex, PETPE (**1**) adopts a conformation unlike either of those observed in its networks with Cu(II). The $-CH_2O-$ spacers that connect each pyridyl group to the core adopt orientations that are no longer nearly fully extended, and the $C_{core}-CH_2-O-C$ dihedral angles have values ranging from 137.92(5)° to 178.44(5)°. As a result, ligand **1** adopts a highly irregular conformation in which the $N\cdots C_{core}\cdots N$ angles vary from 54.67(4)° to 132.39(4)°.

In combination, nominally tetrahedral Cu(I) nodes and tetradentate ligand **1** yield an $SrAl_2$ network (Figure 8a), which can be considered to be constructed from two types of rings, one with a total of four four-connected nodes (alternating Cu and C_{core}) and one with eight four-connected nodes. The average intertectonic $C_{core}\cdots C_{core}$ distance between molecules of ligand **1** that are bonded to a common atom of Cu is 13.367(5) Å, making the network open enough to accommodate 2-fold interpenetration (Figure 8b). Despite this interpenetration, 48% of the volume of the crystals remains accessible to the BF_4^- counterions and to neutral guests.[15−17] The most conspicuous channels run along the *ab* diagonal and have a cross section of approximately 4.4 × 4.4 $Å^2$ (Figure 9).[18]

In forming networks held together by coordination to metals, hydrogen bonds, and weaker interactions, PETPE (**1**) and other pentaerythrityl tetraaryl ethers all display conspicuous flexibility.[13] This compromises their usefulness for constructing materials with predetermined structures and properties. In compensation, however, this flexibility gives ligand **1** and its analogues exceptional versatility in coordination chemistry, by allowing them to accommodate (1) various metals, (2) a single metal in different oxidation states, or (3) a metal in a single oxidation state but with different counterions or secondary ligands, which can have profound effects on the geometry of coordination and on the topology of the resulting networks.[22,23]

Structures of Networks Produced by Treating Extended PETPE (2) with $Cu(NO_3)_2$ and $CuBF_4$. To further probe the usefulness of flexible multidentate ligands for engineering coordination networks, we synthesized tetrapyridine **2**, which extends the $C_{core}\cdots N$ distance in PETPE (**1**) by the insertion of a phenyl spacer. Our goal was to crystallize complexes of analogue **2** with the same three representative salts of Cu(II) and Cu(I) used previously with ligand **1**, so that the resulting structures could be compared directly. Unfortunately, our attempts to grow crystals of a complex of extended PETPE (**2**) with $Cu(OOCCH_3)_2$ were unsuccessful, but after significant effort we were able to crystallize complexes with $Cu(NO_3)_2$ and $CuBF_4$.

Slow mixing of a solution of compound **2** in DMF with an aqueous solution of $Cu(NO_3)_2$ produced blue crystals suitable for analysis by X-ray diffraction (Table 2, Figures 10−12). The crystals proved to have the approximate composition $[Cu(\mathbf{2})(H_2O)_2](NO_3)_2\cdot 2DMF\cdot 6H_2O$.[10] Figure 10 shows that the coordination sphere of Cu(II) is approximately octahedral, with bond angles in the range 87.5(4)−92.5(4)°. The nitrogen atoms of four bound pyridyl groups derived from different molecules of ligand **2** lie in a single plane, and the coordination sphere is completed by two molecules of water bound in a *trans*-diaxial orientation. The average lengths of the Cu−N bonds (2.024(12) Å) and Cu−O bonds (2.450(20) Å) have normal values.[11] The diaxial Cu−O bonds are lengthened conspicuously by Jahn−Teller distortion.[12]

Extended analogue **2** adopts a conformation that holds the four pyridyl groups in an irregular orientation, as shown by $N\cdots C_{core}\cdots N$ angles of 69.6(4)°, 77.7(4)°, 2 × 129.5(4)°, and 2 × 129.9(4)°. The $-CH_2O-$ spacers that connect each pyridylphenyl group to the core adopt conformations that are substantially extended, with $C_{core}-CH_2-O-C$ dihedral angles of 2 × 162.2(11)° and 2 × 165.1(14)°. However, this extension does not continue across the central carbon atom (C_{core}), and the key $CH_2-C_{core}-CH_2-O$ dihedral angles are 2 × 67.2(13)° and 2 × 64.2(13)°. The resulting conformation is closely analogous to the one adopted by PETPE (**1**) itself in its complex with $Cu(NO_3)_2$.

The PtS architecture of the network derived from PETPE (**1**) and $Cu(NO_3)_2$ arises from the combination of two key features: (1) Binding of four pyridyl groups to octahedral Cu(II) in a planar geometry and (2) an extended flattened conformation of PETPE (**1**). These features are unsurprising but not fully predictable, primarily because the geometry of coordination to Cu(II) and the conformation of ligand **1** are

(21) Blake, A. J.; Champness, N. R.; Chung, S. S. M.; Li, W.-S.; Schröder, M. *Chem Commun.* **1997**, 1005–1006. MacGillivray, L. R.; Subramanian, S.; Zaworotko, M. J. *J. Chem. Soc., Chem. Commun.* **1994**, 1325–1326. Nilsson, K.; Oskarsson, Å. *Acta Chem. Scand.* **1982**, *36A*, 605–610.

(22) For a related discussion of the advantages and disadvantages of flexibility in the design of ligands for use in metallosupramolecular chemistry, see: Steel, P. J. *Acc. Chem. Res.* **2005**, *38*, 243–250.

(23) Díaz, P.; Benet-Buchholz, J.; Vilar, R.; White, A. J. P. *Inorg. Chem.* **2006**, *45*, 1617–1626.

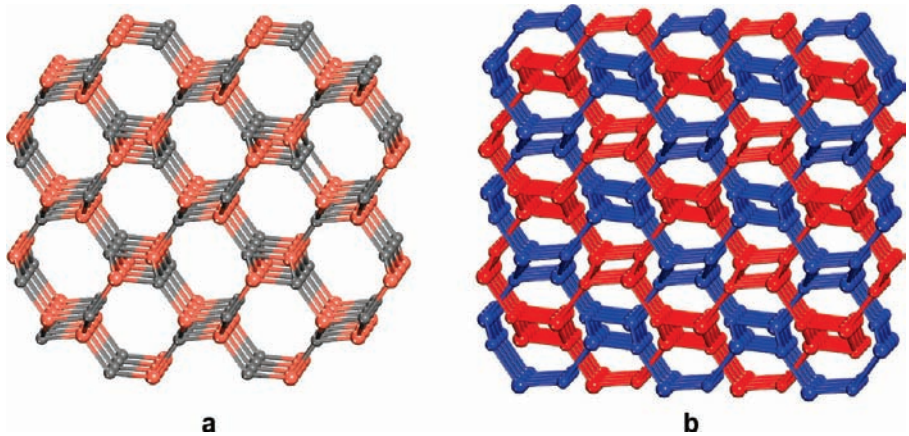

Figure 8. (a) Representation of the $SrAl_2$ network found in crystals of the complex of $CuBF_4$ and PETPE (**1**) grown from CH_2Cl_2/CH_3CN. Nodes in the network correspond to the central carbon atom of ligand **1** (gray spheres) and to Cu(I) (bronze spheres). (b) 2-fold interpenetration viewed along the *a* axis, with one $SrAl_2$ network in blue and the other in red.

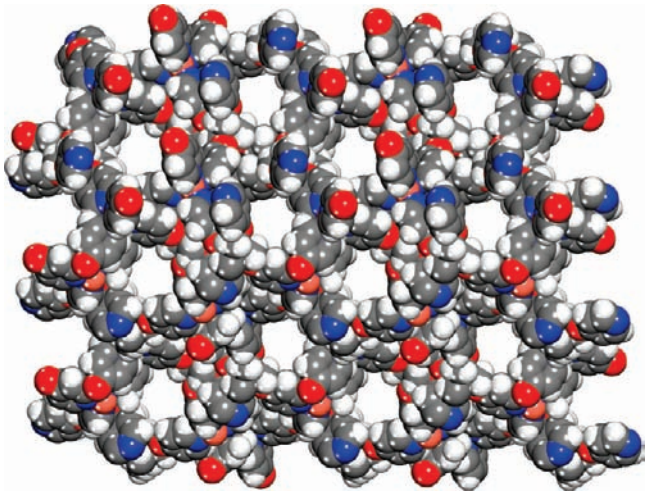

Figure 9. Representation of the structure of crystals of the complex of $CuBF_4$ and PETPE (**1**) grown from CH_2Cl_2/CH_3CN. The structure is viewed along the *ab* diagonal and shows a $1 \times 3 \times 2$ array of unit cells. Anions and neutral guests are omitted for clarity, and atoms are represented by spheres of van der Waals radii to show the cross sections of the channels. Atoms of hydrogen appear in white, carbon in gray, nitrogen in blue, oxygen in red, and Cu(I) in bronze.

Table 2. Crystallographic Data for Complexes of Extended PETPE (**2**) with Salts of Cu(II) and Cu(I)

complex with	$Cu(NO_3)_2$	$CuBF_4$
solvent of crystallization	DMF/H_2O	CH_2Cl_2/CH_3CN
crystal system	orthorhombic	tetragonal
space group	*Pban*	*P4/n*
a (Å)	39.952(5)	15.2141(1)
b (Å)	15.031(2)	15.2141(1)
c (Å)	16.253(2)	13.2235(2)
V (Å^3)	9760(2)	3060.83(5)
D_{calc} (g cm^{-3})	0.835[a]	1.271
Z	4	2
temperature (K)	223(2)	223(2)
unique	9235	3148
observed ($I > 2\sigma(I)$)	3458	3128
parameters	367	201
restraints	38	9
R_1[b]($I > 2\sigma(I)$)	0.0645	0.0422
wR_2[c]($I > 2\sigma(I)$)	0.0876	0.0990
R_1[b](all data)	0.1367	0.0583
wR_2[c](all data)	0.2243	0.1234
GoF[d]	0.863	0.928

[a] Calculated with no solvent included. [b] $R_1 = \sum||F_o| - |F_c||/\sum|F_o|$. [c] $wR_2 = \{\sum[w(F_o^2 - F_c^2)^2]/\sum w(F_o^2)^2\}^{1/2}$. [d] GoF $= \{\sum[w(F_o^2 - F_c^2)^2]/(n-p)\}^{1/2}$, where *n* is the number of reflections and *p* is the total number of parameters refined.

known to vary widely. However, once these features are revealed in the structure of the complex of PETPE (**1**) with $Cu(NO_3)_2$, they provide a basis for expecting extended PETPE (**2**) to behave in a similar way. Indeed, in the complex derived from ligand **2** and $Cu(NO_3)_2$, four pyridyl groups are again bound to Cu(II) in a planar array, and the resulting network has a PtS architecture, now expanded (Figure 11). In this network, the intertectonic $C_{core}\cdots C_{core}$ distance between adjacent ligands (25.401(15) Å) is substantially larger than it is in the PtS network derived from ligand **1** (16.784(9) Å), and the Cu···Cu distance spanned by a single ligand is increased from 16.166(9) Å to 22.838(15) Å. The expanded network is open enough to allow 2-fold interpenetration (Figure 11).

Although the two interpenetrating networks have the same PtS connectivity, they are not identical. Small structural differences appear to optimize $C-H\cdots\pi$ aromatic interactions between the networks.[24] Structures consisting of interpenetrating networks with different geometries or topologies have been observed but are rare.[25] Increases in porosity caused by expansion of the network formed by the reaction of ligand **2** with $Cu(NO_3)_2$ are largely counterbalanced by the effects of interpenetration, and the percentage of volume accessible to disordered nitrate ions and neutral guests rises only from 63% to 66%.[15−17] The resulting network defines interconnected channels that are particularly conspicuous along the *a* axis, the *b* axis, and the *ab* diagonal (Figure 12).[26]

Slow mixing of a solution of extended PETPE (**2**) in CH_2Cl_2/CH_3CN with a solution of $Cu(CH_3CN)_4BF_4$ in CH_3CN produced yellow crystals that could be analyzed by X-ray diffraction (Table 2, Figure 13). The crystals were found to have the approximate composition $[Cu(\mathbf{2})(BF_4)]\cdot$

(24) See the Supporting Information for details.
(25) Baburin, I. A.; Blatov, V. A.; Carlucci, L.; Ciani, G.; Proserpio, D. M. *J. Solid State Chem.* **2005**, *178*, 2452–2474.
(26) Representations of channels were generated by the Cavities option in the program ATOMS Version 6.2 (Shape Software, 521 Hidden Valley Road, Kingsport, Tennessee 37663, U.S.A.; www.shapesoftware.com).

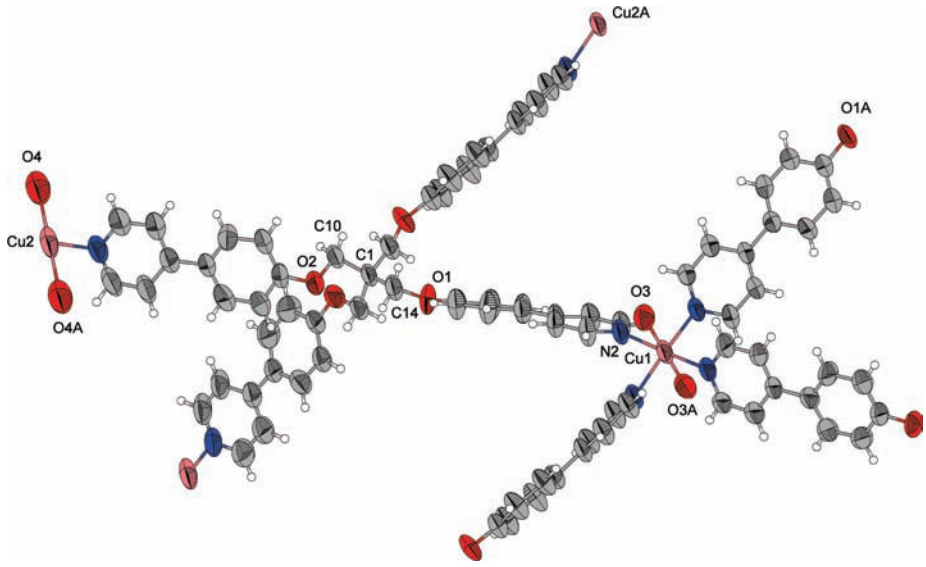

Figure 10. Partial views of the structure of crystals of the complex of $Cu(NO_3)_2$ and extended PETPE (**2**) grown from DMF/H_2O. Thermal displacement ellipsoids are drawn at the 50% probability level, and hydrogen atoms are represented by a sphere of arbitrary size. Atoms of hydrogen appear in white, carbon in gray, nitrogen in blue, oxygen in red, and Cu(II) in bronze. Anions and neutral guests are omitted. Key bond lengths include Cu1−N2 = 2.040(11) Å, Cu2−O3 = 2.409(15) Å, Cu2−N1 = 2.017(14) Å, and Cu2−O4 = 2.50(2) Å.

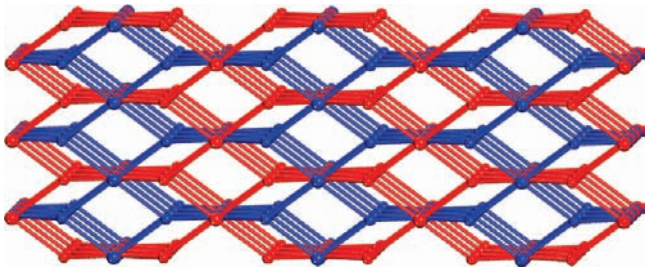

Figure 11. Representation of 2-fold interpenetrated PtS networks found in crystals of the complex of $Cu(NO_3)_2$ and extended PETPE (**2**) grown from DMF/H_2O. The structure is viewed along the *c* axis, with one network in blue and the other in red. Nodes in the networks correspond to the central carbon atom of ligand **2** (small spheres) and to Cu(II) (large spheres).

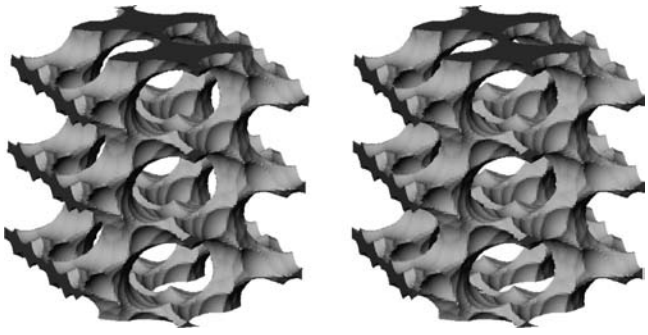

Figure 12. Stereoscopic representation of interconnected channels in the structure of crystals of the complex of $Cu(NO_3)_2$ and extended PETPE (**2**) grown from DMF/H_2O. The images show a 1 × 3 × 2 array of unit cells viewed with the *b* axis vertical. The outsides of the channels appear in light gray, and dark gray is used to show where the channels are cut by the boundaries of the array. The surface of the channels is defined by the possible loci of the center of a sphere of diameter 5.5 Å as it rolls over the surface of the ordered network.[26]

$4CH_3CN \cdot 6H_2O$.[10] Figure 13 confirms that the coordination sphere of Cu(I) is approximately tetrahedral, and the N−Cu−N angles have the values 4 × 103.7(2)° and 2 × 121.8(5)°. The average length of the Cu−N bonds (2.035(10) Å) is normal.[21] Extended PETPE (**2**) favors a conformation that holds the four pyridyl groups in an approximately tetrahedral orientation, with $N\cdots C_{core}\cdots N$ angles of 4 × 106.3(4)° and 2 × 116.0(4)°. The $-CH_2O-$ spacers that connect each pyridylphenyl group to the core adopt conformations that are largely extended, with $C_{core}-CH_2-O-C$ dihedral angles of 169.90(4)°. However, this extension does not continue across the central carbon atom (C_{core}), and the key $CH_2-C_{core}-CH_2-O$ dihedral angles are 66.35(4)°.

Combination of the tetrahedral geometry of Cu(I) with the approximately tetrahedral orientation of the sites of coordination in extended PETPE (**2**) leads to construction of a diamondoid network.[24] In contrast, the pyridyl groups in the Cu(I) complex of simple PETPE (**1**) have an irregular orientation far from the tetrahedral ideal, and a network of $SrAl_2$ topology is formed. Within the network built from ligand **2**, the intertectonic $C_{core}\cdots C_{core}$ distance between adjacent ligands is 20.158(1) Å, and the Cu···Cu distance spanned by a single ligand is 21.516(1) Å. The expanded diamondoid network is open enough to allow 4-fold interpenetration, whereas the $SrAl_2$ network formed from simple PETPE (**1**) and Cu(I) is only 2-fold interpenetrated. The diamondoid network defines parallel channels that run along the *c* axis and have cross sections that are approximately 6.9 × 6.9 $Å^2$.[18,24] About 45% of the volume of the crystals is accessible to included BF_4^- ions, H_2O, and CH_3CN.[15−17]

We were gratified to observe that replacing flexible tetrapyridine **1** with extended analogue **2** yielded networks with identical or related three-dimensional connectivities and with similar geometries of coordination at Cu. In both cases studied, extension of the ligand expanded the resulting network but simultaneously permitted a higher level of interpenetration, so no dramatic increases in the percentage of volume accessible to guests were observed. We reasoned that appropriate substitution of the phenyl spacer in extended PETPE (**2**) might prevent independent interpenetrating networks from approaching closely enough to engage in stabilizing aromatic interactions, thereby leading to lower

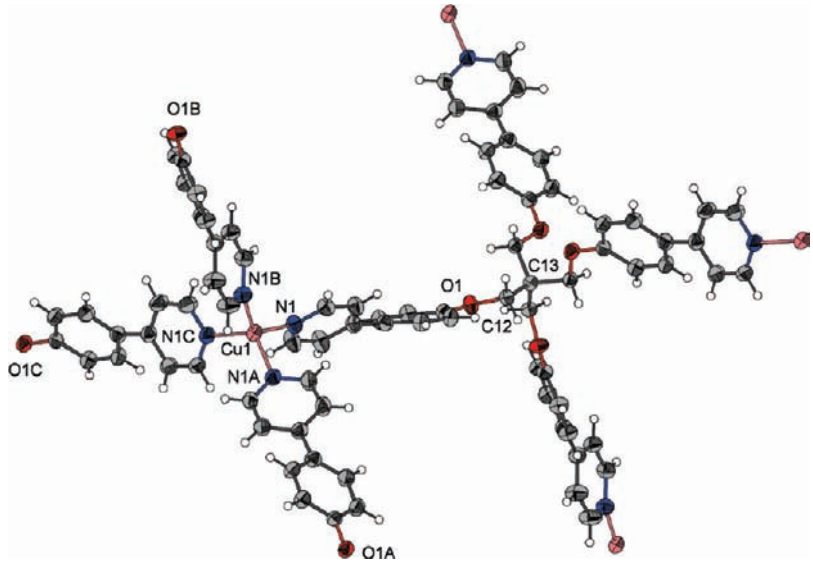

Figure 13. Partial views of the structure of crystals of the complex of $CuBF_4$ and extended PETPE (**2**) grown from CH_2Cl_2/CH_3CN. Thermal displacement ellipsoids are drawn at the 50% probability level, and hydrogen atoms are represented by a sphere of arbitrary size. Atoms of hydrogen appear in white, carbon in gray, nitrogen in blue, oxygen in red, and Cu(I) in bronze. Anions and neutral guests are omitted. Key bond lengths include Cu1−N1 = 2.035-(10) Å.

Table 3. Crystallographic Data for Complexes of Substituted Extended PETPE (**3**) with Salts of Cu(II) and Cu(I)

complex with	$Cu(OOCCH_3)_2$	$Cu(NO_3)_2$	$CuBF_4$	$CuPF_6$
solvent of crystallization	CH_3CH_2OH/CH_3OH	CH_3CH_2OH/CH_2Cl_2	CH_3CH_2OH/CH_3CN	CH_3CH_2OH/CH_3CN
crystal system	tetragonal	cubic	cubic	cubic
space group	$P4_2/n$	$F\bar{4}3c$	$F\bar{4}3c$	$F\bar{4}3c$
a (Å)	30.337(5)	31.7641(11)	32.049(9)	31.9148(8)
b (Å)	30.337(5)	31.7641(11)	32.049(9)	31.9148(8)
c (Å)	7.4230(5)	31.7641(11)	32.049(9)	31.9148(8)
V (Å^3)	6831.6(17)	32048.6(19)	32919(16)	32507.0(14)
D_{calc} (g cm^{-3})	0.744[a]	1.342	1.283	1.395
Z	2	8	8	8
temperature (K)	223(2)	223(2)	293(2)	200(2)
unique	4423	2566	2572	2530
observed ($I > 2\sigma(I)$)	2640	1974	2512	1979
parameters	241	163	167	160
restraints	121	15	5	9
R_1[b]($I > 2\sigma(I)$)	0.0616	0.0628	0.0749	0.0745
wR_2[c]($I > 2\sigma(I)$)	0.1628	0.1502	0.1859	0.1971
R_1[b](all data)	0.0793	0.0643	0.0752	0.0842
wR_2[c](all data)	0.1688	0.1506	0.1859	0.2041
GoF[d]	1.056	1.030	1.162	1.059

[a] Calculated with no solvent included [b] $R_1 = \sum||F_o| - |F_c||/\sum|F_o|$. [c] $wR_2 = \{\sum[w(F_o^2 - F_c^2)^2]/\sum w(F_o^2)^2\}^{1/2}$. [d] GoF = $\{\sum[w(F_o^2 - F_c^2)^2]/(n-p)\}^{1/2}$, where n is the number of reflections and p is the total number of parameters refined.

degrees of interpenetration or to new types of networks, possibly with larger volumes accessible to guests. To test this hypothesis, we prepared methyl-substituted derivative **3** and studied its complexation with Cu(II) and Cu(I), using a representative set of salts that included the same three initially chosen for the complexation of simple PETPE (**1**).

Structures of Networks Produced by Treating Substituted Extended PETPE (3) with $Cu(OOCCH_3)_2$, $Cu(NO_3)_2$, $CuBF_4$, and $CuPF_6$. Blue-green crystals grew during slow mixing of an ethanolic solution of compound **3** with a methanolic solution of $Cu(OOCCH_3)_2$. The crystals were delicate and unstable but could nevertheless be analyzed by X-ray diffraction (Table 3, Figures 14−16). The crystals were found to have the approximate composition $[Cu_2(\mu_2\text{-}OOCCH_3)_4]_2$(**3**).[10] Figure 14 reveals that the structure consists of binuclear paddle-wheel $Cu_2(OOCCH_3)_4$ clusters bridged by axially bound pyridyl groups. The values observed for the length of the Cu−N bonds, the Cu−Cu distance, and the average length of the Cu−O bonds (1.985(6) Å) are closely similar to those found in related binuclear complexes.[27] The pyridyl groups of substituted extended PETPE (**3**) have a distorted tetrahedral orientation, with N···C_{core}···N angles of 4 × 117.3(6)° and 2 × 94.7(6)°. The $-CH_2O-$ spacers that connect each substituted pyridylphenyl group to the core adopt conformations that are substantially extended, with $C_{core}-CH_2-O-C$ dihedral angles of 177.5(12)°.

(27) Yamanaka, M.; Uekusa, H.; Ohba, S.; Saito, Y.; Iwata, S.; Kato, M.; Tokii, T.; Muto, Y.; Steward, O. W. *Acta Crystallogr.* **1991**, *B47*, 344–355. Uekusa, H.; Ohba, S.; Saito, Y.; Kato, M.; Tokii, T.; Muto, Y. *Acta Crystallogr.* **1989**, *C45*, 377–380. Morosin, B.; Hughes, R. C.; Soos, Z. G. *Acta Crystallogr.* **1975**, *B31*, 762–770. Valentine, J. S.; Silverstein, A. J.; Soos, Z. G. *J. Am. Chem. Soc.* **1974**, *96*, 97–103. Kokoszka, G. F.; Duerst, R. W. *Coord. Chem. Rev.* **1970**, *5*, 209–244. Kokoszka, G. F.; Gordon, G. *Transition Metal Chem.* **1969**, *5*, 181–277. Barclay, G. A.; Kennard, C. H. L. *J. Chem. Soc.* **1961**, 5244–5251.

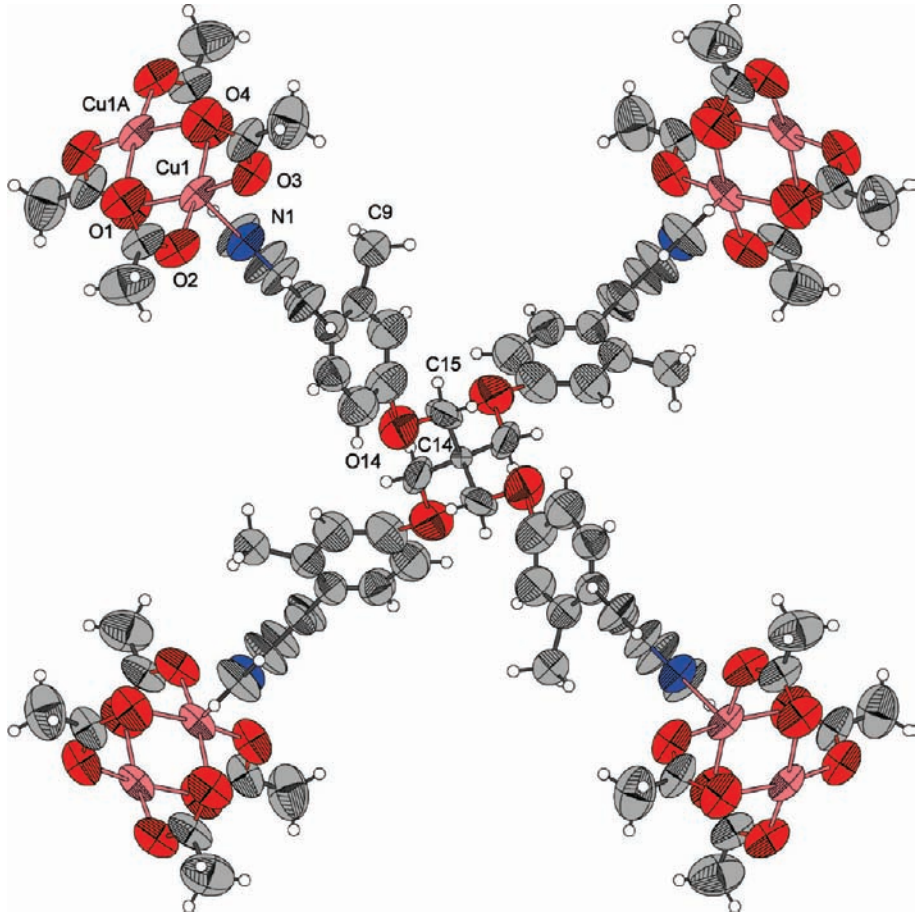

Figure 14. Partial view of the structure of crystals of the complex of $Cu(OOCCH_3)_2$ and substituted extended PETPE (**3**) grown from CH_3CH_2OH/CH_3OH. Thermal displacement ellipsoids are drawn at the 50% probability level, and hydrogen atoms are represented by a sphere of arbitrary size. Atoms of hydrogen appear in white, carbon in gray, nitrogen in blue, oxygen in red, and Cu(II) in bronze. Only one part of the disordered arm of ligand **3** is shown, and guests are omitted. Key bond lengths include Cu1−Cu1A = 2.6460(17) Å, Cu1−O1 = 2.002(6) Å, Cu1−O2 = 1.973(6) Å, Cu1−O3 = 1.965(6) Å, Cu1−O4 = 2.001(6) Å, and Cu1−N1 = 2.193(5) Å.

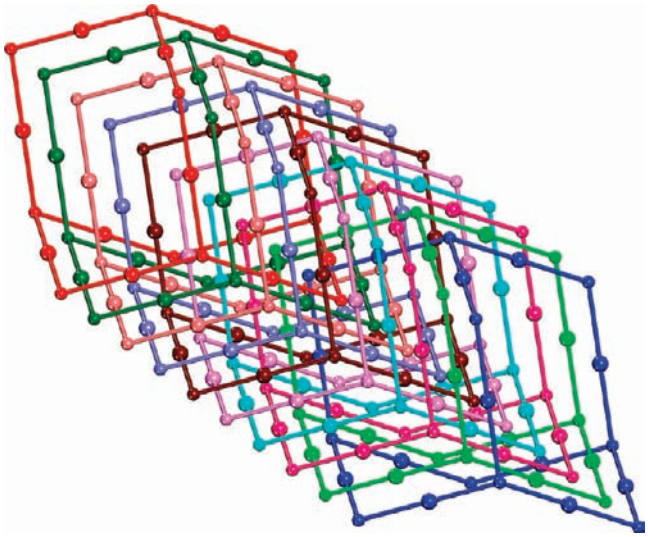

Figure 15. Representation of the 10-fold interpenetrated diamondoid network found in crystals of the complex of $Cu(OOCCH_3)_2$ and substituted extended PETPE (**3**) grown from CH_3CH_2OH/CH_3OH. Nodes and linkers in the network correspond to the central carbon atom of ligand **3** (small spheres) and to the centers of the paddle-wheel $Cu_2(OOCCH_3)_4$ clusters (large spheres).

However, this extension does not continue across the central carbon atom (C_{core}), and the key $CH_2-C_{core}-CH_2-O$ dihedral angles are 53.2(10)°. The resulting conformation closely resembles the one adopted by extended PETPE (**2**) in its complex with $CuBF_4$.

Combination of linear Cu_2 linkers with tetradentate ligand **3** in an approximately tetrahedral conformation yields a diamondoid network. The intertectonic $C_{core}\cdots C_{core}$ distance between adjacent ligands bonded to a common Cu_2 cluster is 28.365(5) Å, and the Cu···Cu distance spanned by a single ligand is 21.862(5) Å. The resulting network is open enough to allow 10-fold interpenetration (Figure 15), yet about 52% of the volume of the crystals remains accessible for the inclusion of guests.[15,16] The guests occupy parallel channels that run along the *c* axis and have cross sections that are approximately 22.7 × 22.7 $Å^2$ (Figure 16).[18] The large size of these channels presumably facilitates the loss of included guests and accounts for the observed instability of the crystals.

It is instructive to compare the networks produced by complexation of $Cu(OOCCH_3)_2$ with PETPE (**1**) and with substituted extended analogue **3**. Both networks are diamondoid, and the extension of ligand **3** helps increase the intertectonic $C_{core}\cdots C_{core}$ distance from 16.731(4) Å to 28.365(5) Å, thereby enlarging the channels significantly. However, interpenetration increases from 5-fold to 10-fold, and the percentage of volume accessible to guests remains

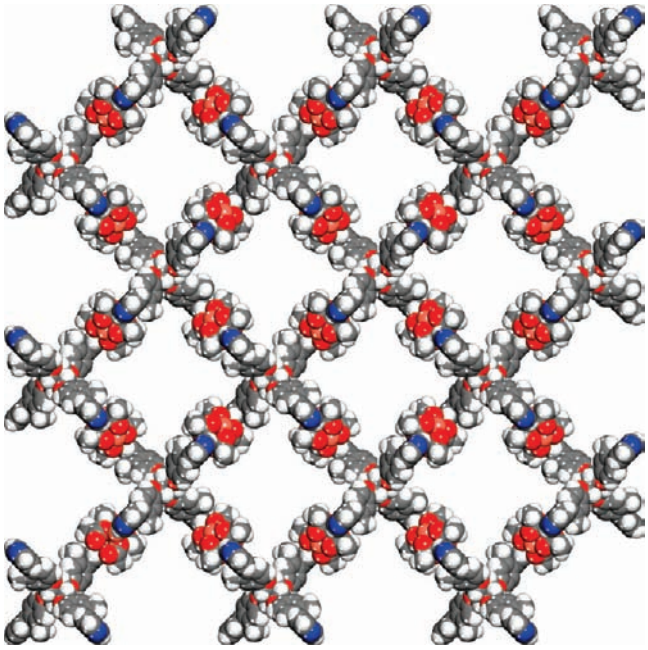

Figure 16. Representation of the structure of crystals of the complex of $Cu(OOCCH_3)_2$ and substituted extended PETPE (**3**) grown from CH_3CH_2OH/CH_3OH. The structure is viewed along the *c* axis and shows a 3 × 3 × 3 array of unit cells. Guests are omitted for clarity, and atoms are represented by spheres of van der Waals radii to show the cross sections of the channels. Atoms of hydrogen appear in white, carbon in gray, nitrogen in blue, oxygen in red, and Cu(II) in bronze.

essentially unchanged. Because ligands **1** and **3** differ both in length and substitution, we cannot determine whether substitution has reduced the degree of interpenetration, as intended, or whether it has helped lead to the incorporation of Cu_2 clusters instead of the simple Cu_1 nodes favored by ligand **1**.

By allowing a solution of compound **3** in CH_2Cl_2 to mix slowly with an ethanolic solution of $Cu(NO_3)_2$, we obtained green crystals that could be analyzed by X-ray diffraction (Table 3, Figures 17−18). The crystals proved to have the approximate composition $[Cu_4(\mathbf{3})_3(H_2O)_{12}](NO_3)_8$[10] and to belong to the unusual cubic space group $F\bar{4}3c$.[28,29] Figure 17 reveals that the coordination sphere of Cu(II) is approximately octahedral and consists of three facially bound pyridyl groups and three molecules of H_2O. The O−Cu−O angles are 63.2(4)°, and the other angles at Cu lie in the range 95.9(3)−98.4(2)°. The average lengths of the Cu−N bonds (2.099(3) Å) and Cu−O bonds (1.923(7) Å) are normal.[11] Ligand **3** adopts a flattened and extended conformation closely similar to the one favored by simple analogue **1** in its complex with $Cu(NO_3)_2$, with N···C_{core}···N angles of 4 × 94.5(4)° and 2 × 147.6(4)°. In both cases, two C−O−CH_2−C_{core}−CH_2−O−C chains are almost fully extended and lie in orthogonal planes.

Joining non-planar 3-connected Cu nodes with 4-connected nodes derived from substituted extended PETPE (**3**) yields a network with a distorted Pt_3O_4 topology. In contrast, analogues **1** and **2** were both found to react with $Cu(NO_3)_2$ to form PtS networks. The new network can be considered to be constructed from rings in which four Cu nodes are linked by four molecules of ligand **3** (Figure 18a). The network is open enough to permit 4-fold interpenetration (Figure 18b), and approximately 20% of the volume of the crystal is accessible for inclusion of disordered counterions and neutral guests.[15,16] No significant channels are defined, and the disordered species instead occupy isolated cavities.[24] Our finding that the complex of $Cu(NO_3)_2$ with ligand **3** does not follow the pattern set by analogues **1** and **2** is consistent with the hypothesis that substitution thwarts interpenetration and thereby directs assembly toward a new topology that can offer a higher density of packing.

To test this notion, we examined networks produced by the reaction of substituted extended PETPE (**3**) with salts of Cu(I). Slow mixing of an ethanolic solution of ligand **3** with solutions of either $Cu(CH_3CN)_4BF_4$ or $Cu(CH_3CN)_4PF_6$ in CH_3CN yielded yellow-green crystals with the approximate composition $[Cu_4(\mathbf{3})_3(CH_3CN)_4](X)_4$ (X = BF_4 or PF_6).[10] To our great surprise, the crystals of both salts proved to belong to the cubic space group $F\bar{4}3c$ and to be isostructural with those of the corresponding complex of $Cu(NO_3)_2$, even though Cu(II) and Cu(I) normally have distinctly different geometries of coordination and therefore give rise to networks with completely different topologies. Crystallographic data appear in Table 3, and views of the coordination sphere of Cu(I) in both salts are shown in Figure 19. Figure 19 establishes that the coordination sphere of Cu(I) is approximately tetrahedral and consists of three bound pyridyl groups and one partially disordered molecule of CH_3CN. In the BF_4^- salt, the N−Cu−N angles have the values 3 × 106.94(8)° and 3 × 111.90(16)°, and the average length of the Cu−N bonds is normal (2.013(8) Å for bound CH_3CN and 2.053(2) Å for the pyridyl groups). Closely similar values are observed for the PF_6^- salt. In both networks, ligand **3** adopts the same flattened and extended conformation found in the complex with $Cu(NO_3)_2$, and again two C−O−CH_2−C_{core}−CH_2−O−C chains are almost fully extended and lie in orthogonal planes.

In the isostructural crystals derived from substituted extended PETPE (**3**), different coordination spheres are observed for Cu(II) and Cu(I), as expected, yet facial binding of three pyridyl groups by octahedral Cu(II) and coordination of three pyridyl groups by tetrahedral Cu(I) generate nodes with similar geometry. A 4-fold interpenetrated network with identical topology (Figure 18) is thereby generated by the reaction of tetrapyridine **3** with Cu(I), and approximately 10% of the volume of the crystals is accessible for inclusion.[15,16] In crystals derived from $CuBF_4$ or $CuPF_6$, the tetrahedral geometry of coordination, the reduced number of ligands bound to Cu, and the lower percentage of volume needed to accommodate counterions all provide strong circumstantial evidence that copper remains in the Cu(I) oxidation state. Additional evidence was obtained by recording diffuse-reflectance spectra of crystalline samples in the UV−visible region. These spectra showed broad reflectance bands at λ = 500−550 nm, which are characteristic of Cu(I).

(28) Of the 415,256 entries in Version 5.28 of the Cambridge Structural Database (including updates),[29] only 2002 structures belong to one of the 35 cubic space groups, and the particular group $F\bar{4}3c$ has merely 37 representatives.

(29) Allen, F. H. *Acta Crystallogr.* **2002**, *B58*, 380–388.

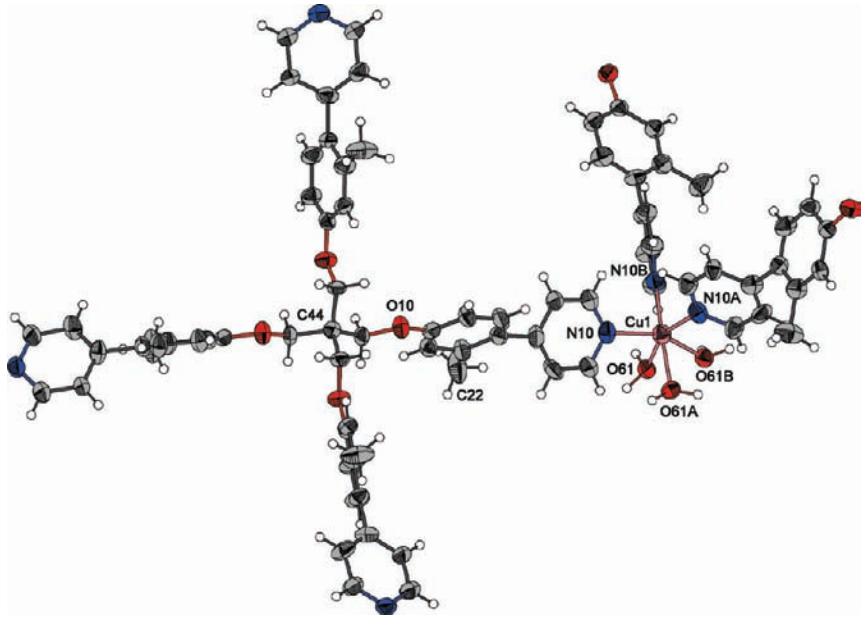

Figure 17. Partial views of the structure of crystals of the complex of $Cu(NO_3)_2$ and substituted extended PETPE (**3**) grown from CH_3CH_2OH/CH_2Cl_2. Thermal displacement ellipsoids are drawn at the 50% probability level, and hydrogen atoms are represented by a sphere of arbitrary size. Atoms of hydrogen appear in white, carbon in gray, nitrogen in blue, oxygen in red, and Cu(II) in bronze. Anions are omitted. Key bond lengths include Cu1−N10 = 2.099(3) Å and Cu1−O61 = 1.923(7) Å.

In contrast, spectra of crystalline samples of the complex of substituted extended PETPE (**3**) with $Cu(NO_3)_2$ showed broad bands at $\lambda < 500$ nm, which are typical of Cu(II).

The cubic networks derived from tetrapyridine **3** have only modest porosity (10−20%) and no obvious channels to permit the exchange of anions or neutral guests.[24] Nevertheless, addition of a solution containing excess $CuPF_6$ in CH_3CH_2OH/CH_3CN to crystals produced by the reaction of ligand **3** with $CuBF_4$ led to quantitative anion exchange, as revealed in IR spectra by disappearance of the BF_4^- peak at 817 cm^{-1} and appearance of a PF_6^- peak at 840 cm^{-1}. Moreover, this exchange occurs without overall loss of crystallinity, as demonstrated by powder X-ray diffraction. These exchanges may occur by sequential dissolution and recrystallization,[30] but the demonstrated ability of ligand **3** to assume different conformations may allow the crystalline networks to flex, thereby facilitating exchange. A similar replacement of PF_6^- by BF_4^- in crystals initially produced by the reaction of ligand **3** with $CuPF_6$ could not be achieved under the same conditions. Greater affinity of the network for PF_6^- may result from its better fit within the cavities of the cubic network.[24]

The feasibility of exchanges, combined with the shared topology of the Cu(II) and Cu(I) networks, suggested that it might be possible to change the oxidation state of copper without loss of crystallinity, thereby producing mixed-valence crystals containing variable ratios of Cu(II) and Cu(I). We attempted to oxidize Cu(I) to Cu(II) in crystals of the complexes of substituted extended PETPE (**3**) with $CuBF_4$ and $CuPF_6$. In these experiments, crystals were exposed under diverse conditions to various oxidants, including H_2O_2, O_2, Br_2, and I_2, but no change in the oxidation state of copper was observed in the solid state.

Conclusions

Our work has demonstrated that tetrapyridines **1**−**3** are effective ligands for the construction of new metal-organic frameworks. Studies of their complexation with Cu(II) and Cu(I) have revealed a distinctive ability to accommodate a single metal in different oxidation states, as well as to adapt to a metal in a single oxidation state but with different counterions or secondary ligands. The adaptability of ligands **1**−**3** arises primarily from their flexibility and ability to assume a set of conformations in which the four pyridyl groups are held in geometries that are approximately tetrahedral, flattened, or irregular. As expected, conversion of simple tetrapyridine **1** into extended analogue **2** by the insertion of phenyl spacers leads to expanded networks. Expansion is accompanied by increased degrees of interpenetration by independent networks, so dramatic increases in porosity are not observed. Attempts to thwart normal interpenetration by converting extended tetrapyridine **2** into substituted derivative **3** were successful, and they yielded complexes that crystallized in the unusual cubic space group $F\bar{4}3c$. Surprisingly, the complexes of ligand **3** with both Cu(II) and Cu(I) gave rise to networks with the same architecture, despite the well-established preference of the two oxidation states of Cu for coordination spheres with different geometries. Together, these results underscore the ability of flexible multidentate ligands to generate metal-organic frameworks with unusual structures and properties. In addition, our observations confirm that interdisciplinary approaches, in which equal attention is devoted to the

(30) Thompson, C.; Champness, N. R.; Khlobystov, A. N.; Roberts, C. J.; Schröder, M.; Tendler, S. J. B.; Wilkinson, M. J. *J. Microscopy* **2004**, *214*, 261–271.

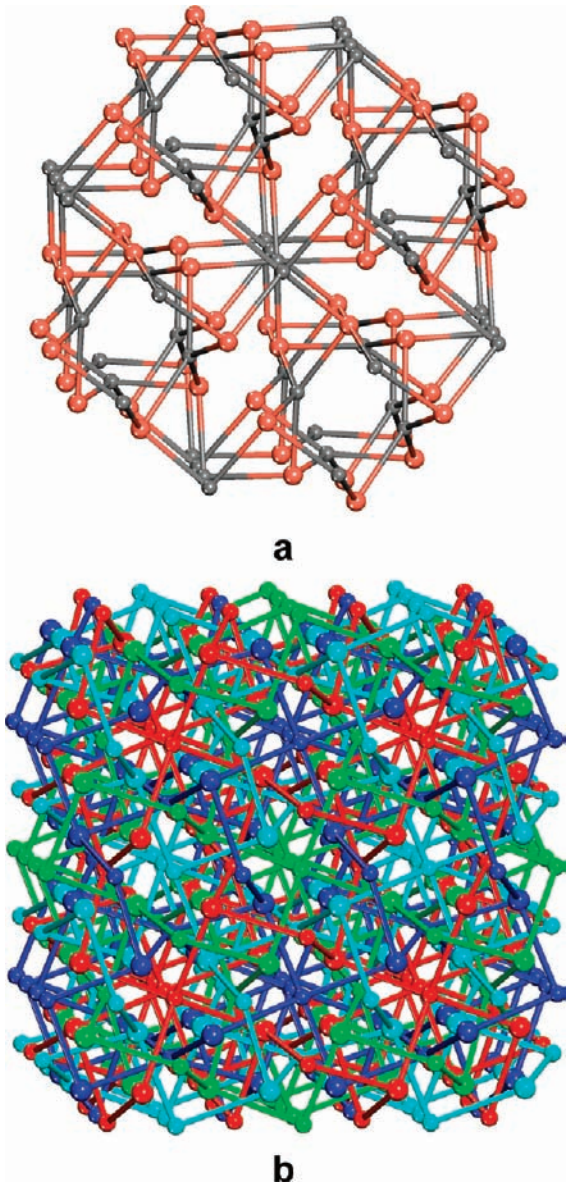

Figure 18. (a) Representation of the Pt_3O_4 network found in crystals of the complex of $Cu(NO_3)_2$ and substituted extended PETPE (**3**) grown from CH_3CH_2OH/CH_3OH. Alternating nodes in the network correspond to the central carbon atom of ligand **3** (gray spheres) and to Cu(II) (bronze spheres). (b) Representation of the 4-fold interpenetrated Pt_3O_4 networks.

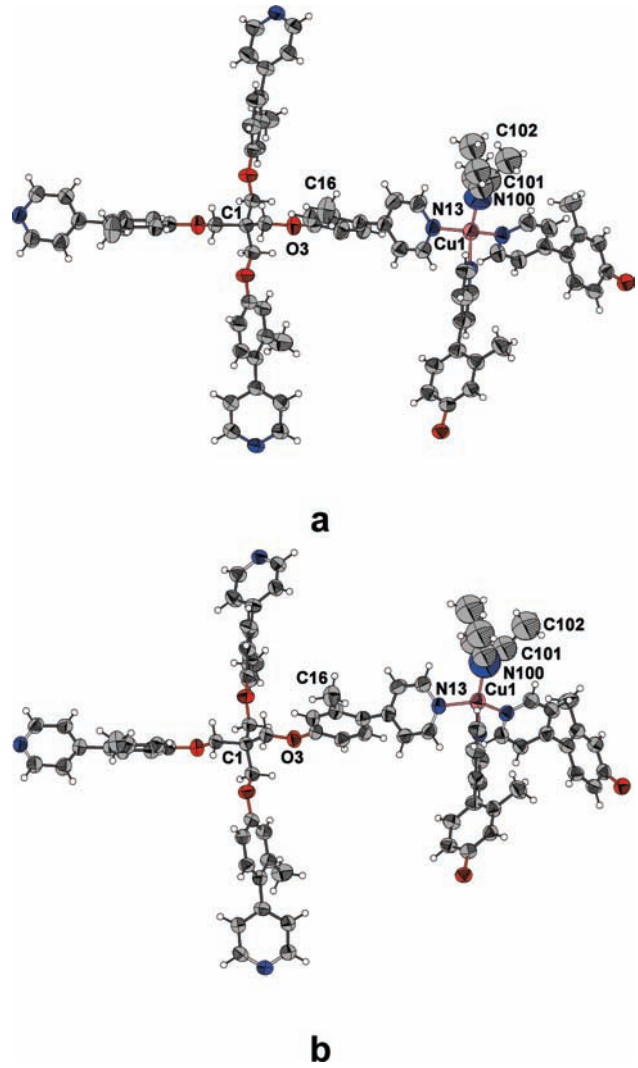

Figure 19. (a) Partial view of the structure of crystals of the complex of $CuBF_4$ and substituted extended PETPE (**3**) grown from CH_3CH_2OH/CH_3CN. Key bond lengths include Cu1−N13 = 2.053(2) Å and Cu1−N100 = 2.013(8) Å. (b) Partial view of the structure of crystals of the complex of $CuPF_6$ and tetrapyridine **3** grown from CH_3CH_2OH/CH_3CN. Key bond lengths include Cu1−N13 = 2.074(4) Å and Cu1−N100 = 2.070(6) Å. Both views show three orientations of disordered CH_3CN coordinated to Cu(I), and anions are omitted. Atoms of hydrogen appear in white, carbon in gray, nitrogen in blue, oxygen in red, and Cu(I) in bronze.

coordination chemistry of metals and to the design and synthesis of complex ligands, are a productive source of new materials.

Experimental Section

All reagents and solvents were purchased from commercial sources and used without further purification unless otherwise indicated. NMR spectra were recorded using a Bruker AV400 spectrometer, and high-resolution mass spectra were obtained using an Agilent LC-MSD TOF spectrometer. Elemental analyses were performed at the Université de Montréal. Diffuse-reflectance spectra were acquired using a Cary 5E UV−vis−NIR spectrophotometer with a Praying Mantis accessory. IR spectra were recorded using a Bruker Vector 22 spectrometer. X-ray diffraction studies were performed with Cu Kα radiation using either (1) a Bruker AXS SMART 2K/Platform diffractometer equipped with a standard sealed X-ray tube or (2) a Bruker AXS SMART 4K/Platform diffractometer equipped with an FR591 rotating anode generator.

Tetrakis[(pyridin-4-yloxy)methyl]methane (1) (PETPE).[5] A mixture of pentaerythritol (0.454 g, 3.33 mmol), 4-chloropyridinium chloride (2.00 g, 13.3 mmol), and NaOH (0.980 g, 24.5 mmol) in DMSO (30 mL) was heated at 60 °C for 72 h. The mixture was then cooled to 25 °C, and water (500 mL) was added. The resulting precipitate was separated by filtration, washed with water, and dried under vacuum to give tetrakis[(pyridin-4-yloxy)methyl]methane (**1**; 1.28 g, 2.88 mmol, 86%) as a colorless solid. An analytically pure sample was obtained by crystallization from toluene: mp 188−190 °C (lit.[5] 198 °C); ^{1}H NMR (400 MHz, $CDCl_3$) δ 8.46 (d, 8H, ^3J = 6.2 Hz), 6.85 (d, 8H, ^3J = 6.2 Hz), 4.41 (s, 8H); ^{13}C NMR (100 MHz, $CDCl_3$) δ 164.2, 151.4, 110.3, 65.7, 44.4; HRMS (FAB, 3-nitrobenzyl alcohol) calcd for $C_{25}H_{25}N_4O_4$ *m/e* 445.18759, found 445.18670. Anal. Calcd for $C_{25}H_{24}N_4O_4$: C, 67.55; H, 5.44; N, 12.60. Found: C, 67.55; H, 5.36; N, 12.49.

Tetrakis[4-(pyridin-4-yl)phenoxymethyl]methane (2) (Extended PETPE). Tetraboronic acid **4** (1.23 g, 2.00 mmol),[8] 4-bromopyridine hydrochloride (1.94 g, 9.98 mmol), $Pd(PPh_3)_4$ (0.464 g, 0.402 mmol), and Na_2CO_3 (2.12 g, 20.0 mmol) were combined under N_2 in a deoxygenated mixture of water and THF (80 mL, 1:3 v/v). The resulting mixture was stirred at 50 °C for 48 h and was then cooled to 25 °C. Water (200 mL) was added, and the mixture was extracted with CH_2Cl_2. The organic phase was dried over anhydrous Na_2SO_4 and filtered, and volatiles were removed by evaporation under reduced pressure. The residual solid was purified by flash chromatography (silica, CH_2Cl_2 (90%)/CH_3CH_2OH (9%)/$N(CH_2CH_3)_3$ (1%), *Rf* 0.42) to yield tetrakis[4-(pyridin-4-yl)phenoxymethyl]methane (**2**; 1.09 g, 1.46 mmol, 73%) as a beige solid: mp 216−217 °C; IR (KBr) 3032, 2933, 2884, 1596, 1518, 1487, 1283, 1244, 1179, 1038, 1016, 815, 756, 628 cm^{-1};^{1}H NMR (400 MHz, $CDCl_3$) δ 8.63 (d, 8H, ^3J = 6.1 Hz), 7.60 (d, 8H, ^3J = 8.8 Hz), 7.45 (d, 8H, ^3J = 6.1 Hz), 7.08 (d, 8H, ^3J = 8.8 Hz), 4.49 (s, 8H); ^{13}C NMR (100 MHz, $CDCl_3$) δ 159.76, 150.43, 147.77, 131.22, 128.39, 121.26, 115.45, 66.75, 45.11; MS (FAB, 3-nitrobenzyl alcohol) calcd for $C_{49}H_{41}N_4O_4$ *m/e* 749.9, found 749.3. Anal. Calcd for $C_{49}H_{40}N_4O_4 \cdot 1.5H_2O$: C, 75.85; H, 5.59; N, 7.22. Found: C, 75.71; H, 5.28; N, 7.07.

4-(4-Methoxy-2-methylphenyl)pyridine (5). (4-Methoxy-2-methylphenyl)boronic acid (3.00 g, 18.1 mmol), 4-bromopyridinium chloride (3.86 g, 19.8 mmol), $Pd(PPh_3)_4$ (0.800 g, 0.692 mmol), and Na_2CO_3 (3.83 g, 36.1 mmol) were combined under N_2 in a deoxygenated mixture of water and CH_3CN (60 mL, 1:3 v/v). The mixture was heated at 80 °C for 72 h and was then cooled to 25 °C. Water (90 mL) was added, and the mixture was extracted with CH_2Cl_2. The organic phase was dried over anhydrous Na_2SO_4 and filtered, and volatiles were removed by evaporation under reduced pressure. The residual oil was purified by gradient column chromatography (silica, $CH_3COOCH_2CH_3$/hexanes (1:9 to 1:1)) to yield 4-(4-methoxy-2-methylphenyl)pyridine (**5**; 3.06 g, 15.4 mmol, 85%) as a colorless solid: mp 70−72 °C; ^{1}H NMR (400 MHz, DMSO-d_6) δ 8.60 (d, 2H, ^3J = 6.0 Hz), 7.35 (d, 2H, ^3J = 6.0 Hz), 7.19 (d, 1H, ^3J = 8.4 Hz), 6.91 (d, 1H, ^4J = 2.5 Hz), 6.88 (dd, 1H, ^3J = 8.4 Hz, ^4J = 2.5 Hz), 3.79 (s, 3H), 2.26 (s, 3H); ^{13}C NMR (100 MHz, DMSO-d_6) δ 160.1, 150.3, 149.4, 137.2, 131.9, 131.4, 125.1, 116.9, 112.6, 55.9, 21.1; MS (ESI, DMSO) calcd for $C_{13}H_{14}NO$ *m/e* 200.1, found 200.1. Anal. Calcd for $C_{13}H_{13}NO$: C, 78.36; H, 6.58; N, 7.03. Found: C, 78.01; H, 6.90; N, 6.99.

3-Methyl-(4-pyridin-4-yl)phenol (6).[9] Aqueous HBr (10.0 mL, 48%) was added to a solution of 4-(4-methoxy-2-methylphenyl)pyridine (**5**; 2.07 g, 10.4 mmol) in acetic acid (10 mL), and the mixture was stirred and heated at reflux for 4 h. The resulting mixture was then cooled to 25 °C, and the pH was raised to ∼ 6.0 by adding aqueous NaOH (6 N). The resulting precipitate was separated by filtration, washed with water, and dried under vacuum. Crystallization from CH_3OH gave 3-methyl-(4-pyridin-4-yl)phenol (**6**; 1.34 g, 7.23 mmol, 70%) as an analytically pure colorless solid: mp 204−206 °C (lit.[9] 206 °C); ^{1}H NMR (400 MHz, DMSO-d_6) δ 9.59 (s, 1H), 8.57 (d, 2H, ^3J = 6.1 Hz), 7.33 (d, 2H, ^3J = 6.1 Hz), 7.08 (d, 1H, ^3J = 8.2 Hz), 6.72 (d, 1H, ^4J = 2.4 Hz), 6.70 (dd, 1H, ^3J = 8.2 Hz, ^4J = 2.4 Hz), 2.21 (s, 3H); ^{13}C NMR (100 MHz, DMSO-d_6) δ 158.4, 150.2, 149.7, 136.9, 131.5, 130.2, 125.1, 118.1, 114.1, 21.1; HRMS (ESI, DMSO) calcd for $C_{12}H_{12}NO$ *m/e* 186.0874, found 186.0934. Anal. Calcd for $C_{12}H_{11}NO$: C, 77.81; H, 5.99; N, 7.56. Found: C, 78.11; H, 5.99; N, 7.60.

Tetrakis{[3-methyl-4-(4-pyridinyl)phenoxy]methyl}methane (3) (Substituted Extended PETPE). Pentaerythrityl tetratosylate (1.08 g, 1.43 mmol)[7] was combined with 3-methyl-(4-pyridin-4-yl)phenol (**6**; 1.33 g, 7.18 mmol) and NaOH (0.288 g, 7.20 mmol) in DMF (15 mL), and the mixture was heated at reflux for 16 h. The resulting mixture was then cooled to 25 °C, and water (200 mL) was added. The resulting precipitate was separated by filtration, washed with water (30 mL) and CH_3CN (30 mL), and dried under vacuum to give tetrakis{[3-methyl-4-(4-pyridinyl)phenoxy]-methyl}methane (**3**; 1.03 g, 1.28 mmol, 90%) as an off-white solid. An analytically pure sample was obtained by crystallization from anhydrous CH_3CH_2OH: mp 260−261 °C; ^{1}H NMR (400 MHz, $CDCl_3$) δ 8.62 (d, 8H, ^3J = 6.1 Hz), 7.22 (d, 8H, ^3J = 6.1 Hz), 7.16 (d, 4H, ^3J = 8.2 Hz), 6.91 (s, 4H), 6.89 (d, 4H, ^3J = 8.2 Hz), 4.45 (s, 8H), 2.28 (s, 12H); ^{13}C NMR (100 MHz, $CDCl_3$) δ 158.9, 149.7, 149.6, 136.9, 132.3, 130.7, 124.6, 117.0, 112.4, 66.5, 45.0, 20.7; MS (FAB+, DMSO) calcd for $C_{53}H_{49}N_4O_4$ *m/e* 805.371, found 805.374. Anal. Calcd for $C_{53}H_{48}N_4O_4$: C, 79.08; H, 6.01; N, 6.96. Found: C, 78.68; H, 6.03; N, 6.93.

Preparation and Crystallization of Complexes. PETPE (1)/$Cu(OOCCH_3)_2$. A solution of $Cu(OOCCH_3)_2$ (33 mg, 0.18 mmol) in CH_3OH (6 mL) was placed in a test tube, and a mixture of CH_3CH_2OH and CH_3OH (12 mL, 1:1 v/v) was carefully layered on top. A solution of PETPE (**1**; 40 mg, 0.090 mmol) in CH_3CH_2OH (2 mL) was then added on top of the other two layers. The tube was sealed, and the contents were allowed to mix slowly. After 2 weeks, blue crystals suitable for X-ray diffraction were obtained.

PETPE (1)/$Cu(NO_3)_2$. A solution of $Cu(NO_3)_2$ hemipentahydrate (42 mg, 0.18 mmol) in water (2 mL) was placed in a test tube, and a mixture of CH_3CH_2OH and water (15 mL, 1:1 v/v) was carefully layered on top. A solution of PETPE (**1**; 40 mg, 0.090 mmol) in CH_3CH_2OH (2 mL) was then added on top of the other two layers. The tube was sealed, and the contents were allowed to mix slowly. After 1 month, violet crystals suitable for X-ray diffraction were obtained. After being dried under vacuum, they had the composition $[Cu(\mathbf{1})(NO_3)_2] \cdot 3H_2O$. Anal. Calcd for $C_{25}H_{30}CuN_6O_{13}$: C, 43.8; H, 4.4; N, 12.2. Found: C, 43.5; H, 4.1; N, 12.2.

PETPE (1)/$CuBF_4$. A solution of PETPE (**1**; 40 mg, 0.090 mmol) in a mixture of CH_3CN and CH_2Cl_2 (7 mL, 6:1 v/v) was placed in a test tube, and CH_3CN (15 mL) was carefully layered on top. A solution of $Cu(CH_3CN)_4BF_4$ (28 mg, 0.090 mmol) in CH_3CN (2 mL) was then added on top of the other two layers. The tube was sealed, and the contents were allowed to mix slowly. After 1 week, yellow crystals suitable for X-ray diffraction were obtained. After being dried under vacuum, they had the composition $[Cu(\mathbf{1})(BF_4)] \cdot CH_3CN \cdot 2H_2O$. Anal. Calcd for $C_{27}H_{31}BCuF_4N_5O_6$: C, 48.26; H, 4.65; N, 10.42. Found: C, 48.28; H, 4.42; N, 10.92.

Extended PETPE (2)/$Cu(NO_3)_2$. A solution of $Cu(NO_3)_2$ hemipentahydrate (25 mg, 0.11 mmol) in water (2 mL) was placed in a test tube, and a mixture of DMF and water (10 mL, 1:1 v/v) was carefully layered on top. A solution of extended PETPE (**2**; 40 mg, 0.053 mmol) in DMF (24 mL) was then added on top of the other two layers. The tube was sealed, and the contents were allowed to mix slowly. After 6 weeks, blue crystals suitable for X-ray diffraction were obtained.

Extended PETPE (2)/$CuBF_4$. A solution of extended PETPE (**2**; 20 mg, 0.027 mmol) in a mixture of CH_3CN and CH_2Cl_2 (7 mL, 6:1 v/v) was placed in a test tube, and CH_3CN (15 mL) was carefully layered on top. A solution of $Cu(CH_3CN)_4BF_4$ (56 mg, 0.18 mmol) in CH_3CN (2 mL) was then added on top of the other two layers. The tube was sealed, and the contents were allowed to mix slowly. After 2 weeks, yellow crystals suitable for X-ray diffraction were obtained. After being dried under vacuum, they had the composition $[Cu(\mathbf{2})(BF_4)]$. Anal. Calcd for $C_{49}H_{40}BCuF_4N_4O_4$: C, 65.45; H, 4.48; N, 6.23. Found: C, 65.95; H, 4.64; N, 6.50.

Substituted Extended PETPE (3)/$Cu(OOCCH_3)_2$. A solution of $Cu(OOCCH_3)_2$ (30 mg, 0.17 mmol) in CH_3OH (10 mL) was placed

in a test tube, and a mixture of CH_3CH_2OH and CH_3OH (10 mL, 1:1 v/v) was carefully layered on top. A solution of substituted extended PETPE (**3**; 30 mg, 0.037 mmol) in CH_3CH_2OH (15 mL) was then added on top of the other two layers. The tube was sealed, and the contents were allowed to mix slowly. After 1 week, blue-green crystals suitable for X-ray diffraction were obtained.

Substituted Extended PETPE (3)/Cu(NO$_3$)$_2$. A solution of substituted extended PETPE (**3**; 30 mg, 0.037 mmol) in CH_2Cl_2 (4 mL) was placed in a test tube, and a mixture of CH_3CH_2OH and CH_2Cl_2 (8 mL, 1:1 v/v) was carefully layered on top. A solution of $Cu(NO_3)_2$ hemipentahydrate (35 mg, 0.15 mmol) in CH_3CH_2OH (4 mL) was then added on top of the other two layers. The tube was sealed, and the contents were allowed to mix slowly. After 3 weeks, green crystals suitable for X-ray diffraction were obtained.

Substituted Extended PETPE (3)/CuBF$_4$. A solution of substituted extended PETPE (**3**; 30 mg, 0.037 mmol) in CH_3CH_2OH (4 mL) was placed in a test tube, and a mixture of CH_3CN and CH_3CH_2OH (6 mL, 1:1 v/v) was carefully layered on top. A solution of $Cu(CH_3CN)_4BF_4$ (47 mg, 0.15 mmol) in CH_3CN (5 mL) was then added on top of the other two layers. The tube was sealed, and the contents were allowed to mix slowly. After 1 week, yellow-green crystals suitable for X-ray diffraction were obtained. After being dried, they had the composition $[Cu_4(\mathbf{3})_3](BF_4)_4$. Anal. Calcd for $C_{159}H_{144}B_4Cu_4F_{16}N_{12}O_{12}$: C, 63.31; H, 4.81; N, 5.57. Found: C, 63.53; H, 4.68; N, 6.04.

Substituted Extended PETPE (3)/CuPF$_6$. A solution of substituted extended PETPE (**3**; 30 mg, 0.037 mmol) in CH_3CH_2OH (4 mL) was placed in a test tube, and a mixture of CH_3CN and CH_3CH_2OH (6 mL, 1:1 v/v) was carefully layered on top. A solution of $Cu(CH_3CN)_4PF_6$ (56 mg, 0.15 mmol) in CH_3CN (7 mL) was then added on top of the other two layers. The tube was sealed, and the contents were allowed to mix slowly. After 1 week, yellow-green crystals suitable for X-ray diffraction were obtained.

X-ray Crystallographic Studies. Intensity data were collected with 0.3° width ω scans to get a full sphere of reciprocal space. Data were processed using SAINT software.[31] Data reduction included absorption corrections by the multiscan method with SADABS software.[32] Crystallographic data, data collection parameters, and structure refinement details are given in Tables 1−3. Structures were solved by direct methods and refined by full-matrix least-squares techniques.[33] Except in the case of one structure with severe disorder, all non-hydrogen atoms were refined with anisotropic displacement parameters. Hydrogen atoms were placed at calculated positions and refined as riding atoms in the subsequent least-squares model refinements, except for certain hydrogen atoms of water molecules that were located by the Fourier difference map or placed at positions to favor hydrogen bonding, then refined using restraints on distances and angles. The isotropic thermal parameters were estimated to be 1.2 (1.5 for methyl hydrogens) times the values of the equivalent isotropic thermal parameters of the non-hydrogen atoms to which hydrogen atoms are bonded. Counterions and neutral guests were usually located and refined using multisite models for disorder, except for two structures that were found to have large voids filled with disordered anions and neutral guests, which could not be modeled in a satisfactory way. In these cases, the SQUEEZE option implemented in PLATON was used to account for the contribution of the disordered guest.[16] More information about structural refinement is provided in the CIF files available as Supporting Information.

Acknowledgment. We are grateful to the Natural Sciences and Engineering Research Council of Canada, the Ministère de l′Éducation du Québec, the Canada Foundation for Innovation, the Canada Research Chairs Program, and Université de Montréal for financial support. We thank Dr. Alexandra Furtos and Karinne Venne for obtaining mass spectra, Dr. Christian Reber and Valérie Baslon for helping us record UV−visible diffuse-reflectance spectra, and Prof. Jurgen Sygusch for providing access to a diffractometer equipped with a rotating anode.

Supporting Information Available: Additional structural views and crystallographic details (CIF files) for the complexes of Cu(II) and Cu(I) with ligands **1**−**3**. This material is available free of charge via the Internet at http://pubs.acs.org.

IC8019809

(31) *SAINT-Plus, Versions 6.35A and 7.34a*; Bruker AXS Inc.: Madison, WI, 2002, 2006.

(32) Sheldrick, G. M. *SADABS, Versions 2.05 and 2007/2*; University of Göttingen: Göttingen, Germany, 2002, 2007.

(33) Sheldrick, G. M. *Acta Crystallogr.* **2008**, *A64*, 112–122.